The potential and cost of carbon dioxide removal using direct air capture with land-based wind and utility-scale photovoltaics

Elwin Hunter-Sellars,[a]‡ Tao Dai,[b,c]‡ Nathan C. Ellebracht,[a] Hélène Pilorgé,[d] Maxwell Pisciotta,[d] Alexander P. Bump,[e] Edna Rodriguez Calzado,[e] Susan D. Hovorka,[e] Corinne D. Scown,[b,c,f,g] Simon H. Pang[a],**

[a] Materials Science Division, Lawrence Livermore National Laboratory, Livermore, CA, USA

[b] Biological Systems & Engineering Division, Lawrence Berkeley National Laboratory, Berkeley, CA, USA

[c] Joint BioEnergy Institute, Emeryville, CA, USA

[d] Department of Chemical and Biomolecular Engineering, University of Pennsylvania, Philadelphia, PA, USA

[e] Bureau of Economic Geology, The University of Texas at Austin, Austin, TX, USA

[f] Energy Analysis & Environmental Impacts Division, Lawrence Berkeley National Laboratory, Berkeley, CA, USA

[g] Energy & Biosciences Institute, University of California, Berkeley, Berkeley, CA, USA

KEYWORDS. Carbon capture, renewable electricity, geologic storage, geospatial analysis, technology learning

ABSTRACT

Rapid deployment of direct air capture and storage (DACS) is essential for meeting net-zero emission targets and requires accurate assessment of both the scale and cost of carbon dioxide removal. This analysis, focused on land, renewable electricity, and geologic CO_2 storage availability within the United States, estimates a technical potential capacity for low-temperature, adsorbent DACS of approximately 9 gigatonnes of CO_2 per year. Much of this removal could be accomplished at costs between $200–250 per tonne of CO_2, depending on the scale and location of the facility, and the associated storage costs. High-potential regions were identified in West Texas, the Rocky Mountains, and Alaska, among others. In the near term, DACS deployment will identify critical research areas for technology improvement to reduce the cost of carbon removal; simultaneously, there is a need for scientifically guided and rigorous standards for DACS monitoring, reporting, and verification across existing and emerging DACS technologies and energy sources.

1. INTRODUCTION

Reaching global carbon neutrality will require, beyond mitigation of existing greenhouse gas emissions, rapid and expansive deployment of carbon dioxide removal technologies to compensate for hard-to-abate emissions and eventually address historic anthropogenic emissions. Recent reports suggest the United States alone will require carbon removals at the gigatonne scale by 2050 [1,2], likely achieved through a combination of nature- and engineering-based solutions [3,4]. To bridge the gap in the scale and durability of nature-based carbon dioxide removal (CDR) solutions [2], such as afforestation and soil carbon sequestration, more costly and upcoming engineering-based removals will be required, with direct air capture and storage (DACS) being one the most widely studied [5].

The majority of DACS technologies deployed today can be grouped into two categories. The first is solvent-based DACS, which puts incoming air in contact with a liquid solvent, such as an aqueous hydroxide, which reacts with CO_2 to form a carbonate [6]. The carbonate, following several processing steps, is eventually treated at temperatures approaching 900 °C to release the high purity CO_2 for storage. The high regeneration temperature is typically accomplished via oxycombustion of natural gas [6], although electrified kilns may provide a solution less reliant on fossil fuels, provided their scale limitations can be overcome [7]. The use of a solvent capture agent also leads to substantial evaporative water losses, estimated at 1–9 tonnes water per tonne of captured CO_2 [6]. The second option, adsorbent-based DACS, commonly uses functionalized solids in a two-step 'swing' process in which the solid chemically binds CO_2 before being regenerated to release it [8]. This regeneration occurs at temperatures between 80–120°C, allowing for a greater diversity of heat sources, which in turn enables integration with low-carbon and renewable energy sources. While there are several emerging approaches to DACS, both in terms of the method of

capture (mineral adsorption [9,10], physisorbents [11]) and regeneration (moisture-[12], pH-[13], electro-swing[14]), the lack of in-depth cost and process information available to-date makes their assessment for large-scale deployment difficult at this time.

Regardless of the specific technology utilized, DACS deployment must ramp up considerably to reach the net-zero goals of the United States, requiring significant investment in terms of land, energy, natural resources, and capital. Due to DACS' high energy requirements, approximately 80% of which is used for regeneration heat [15,16], rapid expansion requires concurrent expansion of energy generation. Renewable electricity is perhaps the most promising power source for DACS due to its low cost and low carbon intensity, high scalability, and siting flexibility [17]. Adsorbent DACS is particularly suited to utilize on-site renewables as it can be operated entirely via electricity through the use of Joule heating [18,19], electric boiler-produced steam [16], or electric heat pumps [8]. In this configuration, the majority of the land footprint is occupied by electricity generation [20,21], with the capture facility itself expected to only account for less than 2% of the total land area [8,20]. Alongside electricity requirements, deployment of DACS is limited by the storage potential of geologic formations in proximity to the capture facility. Estimations of geologic CO_2 storage potential in the United States are in the thousands of gigatonne scale [22,23] but is highly spatially dependent [2], requiring combined capture and storage on-site or the use of CO_2 pipeline infrastructure.

Most current studies on DACS deployment focus on what is required instead of what is possible within different timeframes. In the early years of deployment, coined the 'formative phase' by Nemet et al. [24], novel forms of CDR will need to grow rapidly to become climate relevant, as widespread deployment will allow CDR to benefit from factors such as technology learning rates [25], market competition [26], and public-private partnerships [26]. Nemet's analysis suggests that,

depending on the scale of DACS relative to other novel CDR technologies, hundreds of facilities, each capturing 1 megatonne of CO_2 per year, may be required by 2040 to reach gigatonne-scale for net-zero by mid-century. Actual assessments of possible near- and long-term deployment of DACS focus on the availability of electricity and heat to operate the facility, and their co-location or proximity to geologic storage [23,27].

Work by Young et al. [26] estimated the evolving costs of a DACS facility, and a facility where gigatonne scale had been reached. In the near-term, location drives variation in DAC prices due to differences in labor and materials costs, while in the long-term the electricity source becomes more critical due to decreasing capital costs with deployment. The report estimates that solid adsorbent DACS will cost between \$170–730 per tonne of net-removed CO_2, which is in agreement with other assessments [28], and that grid decarbonization should be a priority both for reducing emissions and for powering DACS. Fauvel et al. [29] suggest that DACS could have a significant demand on both regional electricity generation and natural gas supplies by 2050, but could still play a significant role alongside other negative emissions technologies depending on its cost at scale. Geothermal energy has been identified as a potential accelerator for near-term adsorbent DAC deployment, with McQueen et al. [16] estimating removal potentials between 10–13 megatonnes of CO_2 per year in the United States alone, at costs below \$300 per tonne of CO_2. However, the global potential for DACS powered by geothermal energy has been estimated at only 1 gigatonne of CO_2 per year by Fahr et al [30], several orders of magnitude lower than the potential for wind- or solar-powered DACS. A study by Terlouw et al. [27] came to similar conclusions regarding the utilization of industrial waste heat for DACS in Europe, with only Sweden having enough capacity to feasibly compensate for 10% of its national emissions through waste-heat powered DACS. These studies

illustrate the need for accurate assessment of DACS potential capacity and cost, and how these are influenced by the location of the facility, and the timeframe in which it is deployed.

In this study we investigated the near- and long-term deployment of adsorbent-based DACS within the United States utilizing renewable electricity. High-resolution geospatial analysis was used to identify the intersection between: 1) available land, accounting for physical (land category, slope) and social (protected lands) constraints; 2) available electricity, including construction of on-site renewable energy generation while accounting for electricity needs for grid decarbonization; 3) identified and quantifiable geologic storage. Spatially explicit capture costs and potentials were quantified at the United States county level, highlighting regions of high opportunity for large-scale adsorbent DACS deployment. Current grid electricity mixes were assessed to understand their role in DACS deployment. This work lays the groundwork for, and emphasizes, the importance of further in-depth regional studies, moving away from a 'one size fits all' solution for carbon dioxide removal.

2. METHODS

2.1. CO_2 capture facility process model

For the adsorbent DACS process, a process model was developed based on a modular vacuum-temperature-swing system using an amine-based adsorbent loaded onto a square-channel contactor (**Figure 1**) [2,16]. The model assumes a fixed cycle time and working CO_2 capacity, the latter of which was modulated by local temperature and humidity [31] and set to decrease at due to degradation of the amine-based adsorbent [32]. The heat for regeneration was supplied via steam generated by a renewable electricity-powered heat pump. A full summary of the process parameters can be found in **Table S1**.

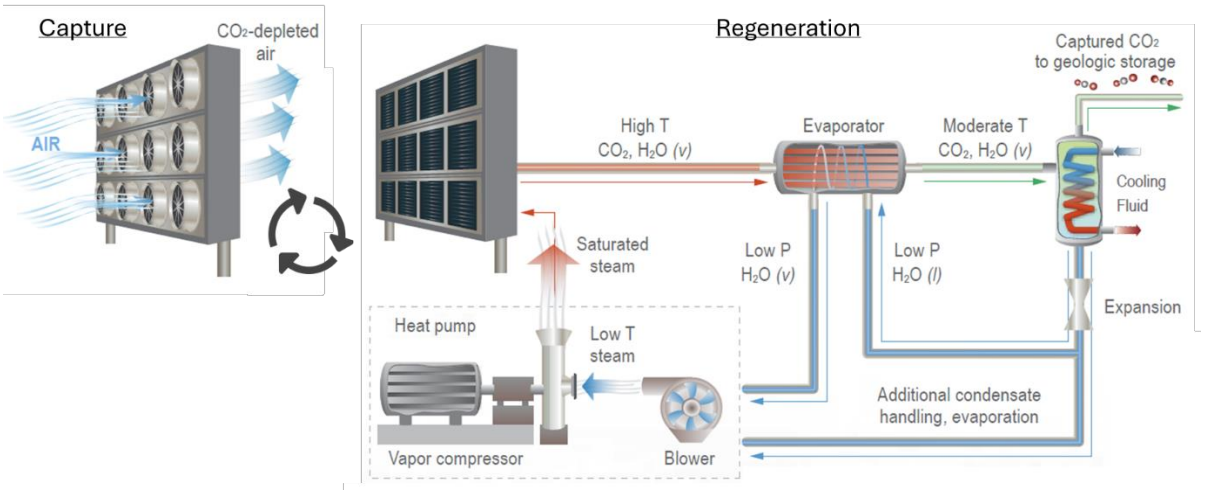

Figure 1. Schematic of mass and heat flow within adsorbent DAC process, wherein heat is provided via saturated steam, itself generated using an electric heat pump [2]. The heat pump system, powered by grid or renewable electricity, may receive heat input from the evaporator or available low-grade heat or air. Captured CO_2 is sent for refining and compression prior to geologic storage (not pictured). Adapted from Pett-Ridge et al. [2]

We evaluated two timepoints for adsorbent DACS deployment. In the near-term (2025), energy was assumed to be supplied by grid electricity, with the cost and carbon intensity of this electricity varying by state (**Table S2**) [33 34]. The facility was assumed to be co-located with geologic storage, the cost of which was based on long-term projections of storage cost [2]. Environmental conditions of 15°C and 55 % relative humidity were used for productivity estimates.

For adsorbent DACS deployment in 2050, a learning-by-doing analysis was carried out based on the estimated deployment of adsorbent DACS by 2025 [35–37]. The levelized cost of carbon removal was estimated by projecting capital costs based on estimations of total global deployment in 2050, and projecting operating costs using state-level electricity prices, which in turn were based on a 100% grid decarbonization scenario [38] (**Table S2**). The climate-dependent productivities were

used to calculate the quantity of adsorbent required to match the capture demands dictated by renewable energy supply, rather than affecting the scale of the facility.

2.2. Long-term potential and cost of renewable-powered adsorbent-DACS

Technical potential and cost estimates for 2050 were based on the assumption that future DACS development would utilize on-site renewable electricity, constraining capture potential by land availability, electricity generation potential, and proximity to geologic storage.

2.2.1. Suitable land analysis

Due to the small land footprint of an adsorbent DACS facility, the land suitability analysis was focused on what is required for land-based wind and utility-scale photovoltaics, chosen based on their projected low cost compared to other forms of renewable energy [39].

Land suitability criteria categorized into 'general' restrictions agnostic to the generation technology, and 'specific' restrictions that account for the unique requirements of each technology. These restrictions, summarized in **Table S3**, were applied onto the 30-meter resolution 2019 National Land Cover Database (NLCD) [40]. The NLCD layer, due to its high resolution, serves as a reference layer of projection and processing steps for any geospatial analysis.

General siting criteria were grouped into three categories. The first, land classification, excluded lands categorized as 'water' or 'wetlands', including a buffer region for the latter due to the difficulty of constructing electricity generation and capture facilities on these lands. The second, developed lands, excluded land categorized as 'developed' and applied buffer zones around man-made installations such as buildings, airports and power plants. The third excluded lands identified as 'protected' by United States Government, such as wilderness areas, national parks, and historic areas due to the potential ecological and societal harm that DACS construction could have in these areas.

Technology-specific criteria were then applied, based on the highest generation potential for each region. The first excluded land with slope equal above 5 and 20% for wind and solar respectively. The second excluded land based on their co-location with certain NLCD land classes. This was accomplished by grouping the land class data, at 30-meter resolution, into 2250 by 2250 meter (~5 km^2) analysis spaces. Wind development was excluded in spaces containing more than 25% forest, and solar development in areas with more than 25% of forest, pasture/hay, or cultivated crops [40]. The third criteria excluded land that is projected to be occupied by wind/solar development for United States electrical grid decarbonization as identified by Denholm, *et al.* [41] in the "All-Options" which included DACS deployment as part of its analysis. It is important to note that future demands for grid and/or renewable electricity, such as those required for data centers and emerging technologies such as artificial intelligence [42,43] could require significant expansion of renewable electricity generation, but were not included in this analysis due to their difficulty to predict. Finally, a minimum contiguous land area of 5km^2 was specified to remove isolated pixels. In Alaska, solar photovoltaic was excluded as a primary renewable energy option because of low solar resources in that region [44].

After determining suitable land, the 30-meter resolution map was resampled into a 2250-meter resolution grid point map (**Figure S1**). We consider this an acceptable tradeoff to improve computational efficiency due to the minimum land contiguous area requirement of 5 km^2.

2.2.2. Renewable electricity potential and cost analysis

At each of the resampled grid points *i*, the electricity generation potential $E_{i,j}$ in MWh per year with technology *j* (*j* is wind or solar) can be calculated as:

$$E_{i,j} = CF \times 8760 \times A_{i,j} \times PD_j$$

where CF is the capacity factor, $A_{i,j}$ is the quantity of suitable land, in km^2, and PD_j is the power density of the technology, 4.3 [45] and 45 [46] MW per km^2 for wind and solar respectively.

2.2.3. Geologic storage potential and cost

For this analysis, adsorbent DACS facilities were assumed to be constructed only on land with geologic storage potential. While CO_2 transport has been considered using several methods [47], it is beyond the scope of this work. Spatially explicit geologic storage capacities and cost were taken from Chapter 4 of the 'Roads to Removal' report [2], which took into account factors related to injectivity, CO_2 plume and pressure area, and the costs associated with project exploration. Regions with poorly defined storage potential or cost, and electricity generation grid points overlapping these regions, were excluded from further analysis.

2.2.4. Impact of local climate on performance

To quantify the impact of climate—temperature and humidity/dew point—on capture productivity, spatially explicit climate data at a resolution of 25 kilometers [48] was combined with estimates of productivity at different temperatures and dew points [31], adapted to adjust the cyclic working capacity of the adsorbent.

3. RESULTS AND DISCUSSION

3.1. Near-term cost of adsorbent DACS

At a plant scale of 0.3 megatonnes of CO_2 per year, we estimate that a first-of-a-kind adsorbent DACS facility could capture and store CO_2 at a cost of $630 per tonne CO_2, in good agreement with the cost ranges estimated by previous studies [26,28]. The overall cost is most strongly affected by the capital cost for adsorbent material and regeneration, and the electricity costs associated with the steam generation, calculated as the average of state-level industrial prices in 2025 [33]. This cost is a 'net-removed' cost and is highly dependent on the carbon intensity of the heat and electricity

(i.e. the CO_2 released during heat and electricity generation, **Figure S2**). For example, if natural gas is used for steam generation without capturing the combustion emissions, the cost of capture increases to $800 per tonne of CO_2 due to the subsequent release of CO_2 during natural gas combustion (**Figure S3**).

3.1.1. Impact of electrical grid carbon intensity

Due to the high energy requirements of adsorbent DACS, the carbon intensity of the grid electricity also strongly affects the net-removed cost of CO_2 capture. These carbon intensities vary strongly by state (**Figure 2**) due to differences in energy source and power plant efficiency. Based on 2021 grid carbon intensity, two states (Washington and Vermont) could capture CO_2 at below $500 per tonne of CO_2, although the lack of availability of geologic storage in these regions makes deployment challenging. In states like Wyoming and Indiana, where most electricity is generated through coal or natural gas, CO_2 emissions from electricity generation exceed the quantity of CO_2 captured by DACS, resulting in overall positive emissions and effectively 'infinite' net-removed cost. Similar results were demonstrated by Sendi et al. [49] who found that net CO_2 removal could not be achieved in India, China, South Africa, and the central United States due to their grid carbon intensity. This demonstrates the need for carefully considering the CO_2 emissions of a region's existing electrical grid mixture if DACS is planned to utilize it and illustrates the importance of grid decarbonization.

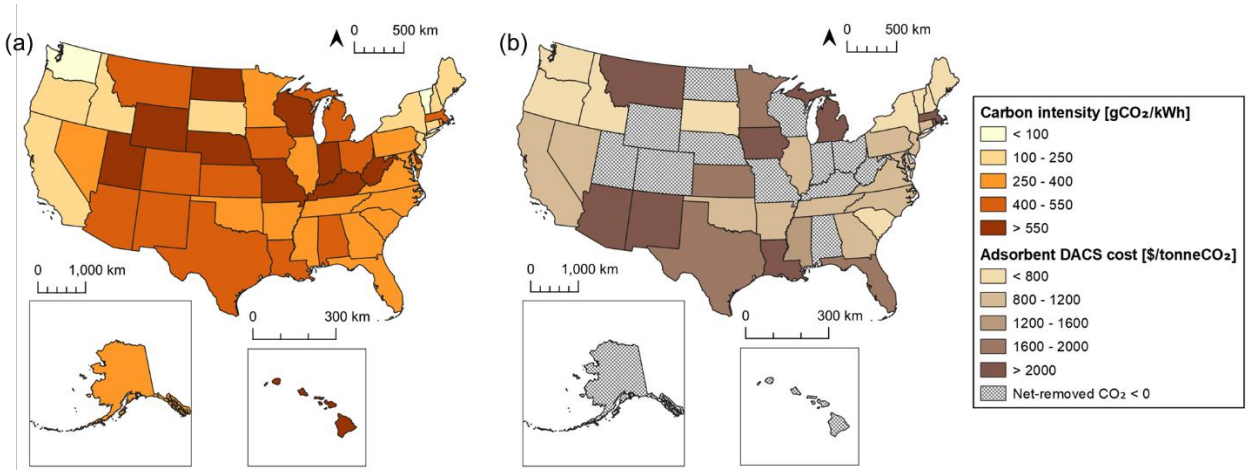

Figure 2. (a) State-level carbon intensities of 2021 electrical grid; (b) State-level Costs for adsorbent DACS facilities powered by equivalent grid electricity. Calculations assume facility size of 0.3 megatonnes of CO_2 per year.

3.2. Long-term deployment of renewable-powered adsorbent DACS

3.2.1. Identifying suitable land for renewable energy generation

As shown in **Figure 3(a)**, the criteria that resulted in the largest above-ground land exclusions were regions with excessive slope (0.53/ 1.69 million km^2 for wind/solar), regions containing or adjacent to wetlands (1.74 million km^2), and land prioritized for grid decarbonization (1.07/ 0.67 million km^2 for wind/solar). Exclusion type was strongly related to the NLCD land classification within a region. For example, forests and shrublands made up approximately 38 and 35 % of protected lands, but only 27 and 7 % of lands on or around wetlands respectively.

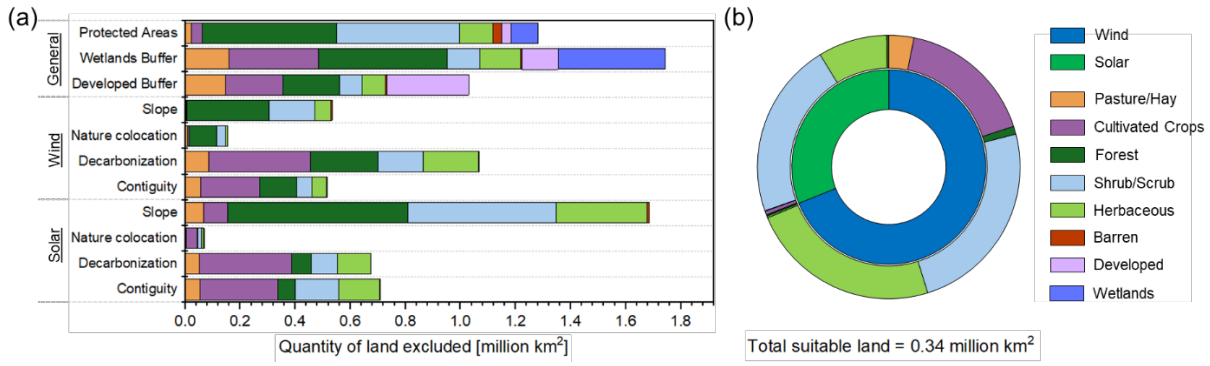

Figure 3. (a) Quantity of land excluded by general and technology-specific above-ground siting criteria; (b) land-class distribution of area intersecting renewable generation and geologic storage.

After applying above-ground general and technology-specific siting criteria (**Figure S4**), approximately 1.2 million km^2 was identified as suitable for renewable electricity generation, with 0.45 and 0.75 million km^2 being utilized for solar and wind respectively. States surrounding, or east of, the Rocky Mountains such as Montana and Wyoming have high potential for wind, as does north and southwest Alaska, while southwestern states such as Texas, New Mexico, and Arizona have high potential for solar. These analyses were conducted at a 30-meter resolution, higher than other studies analyzing siting of wind [50,51] and solar [51] electricity generation, with resolutions between 90-100 meters, which can lead to differences in the determined quantity of suitable land (**Figure S5**), and results in a more conservative estimate of the quantity of suitable land for electricity generation.

3.2.2. Intersection with geologic storage

When considering only generation above geologic storage with quantifiable cost and capacity, approximately 0.34 million km^2 could be utilized for renewables generation for adsorbent DACS (**Figure 3(b)**). This land accounts for 16% of the total land area in the contiguous United States and would enable the generation of 41 and 10 PWh by solar and wind installations respectively.

In regions where both wind and solar energy could be produced, the technology with the higher generation potential was prioritized, although selecting based on cost produced similar results (**Figure S6**). Much of this land is of the 'Herbaceous' or 'Shrub/Scrub' land class, and is located in south and west Texas, Wyoming, and Colorado, with storage costs per tonne of CO_2 varying between $4–40, with an average of $8. The requirement for collocation with geologic storage eliminated several regions within the western United States with significant potential for renewable electricity generation, such as northern Nevada and southern Arizona—both of which, due to their low population density, have relatively little land prioritized for decarbonizing the electrical grid [41]. These regions demonstrate the benefits of expansive mass and energy transport networks for both grid decarbonization and direct air capture.

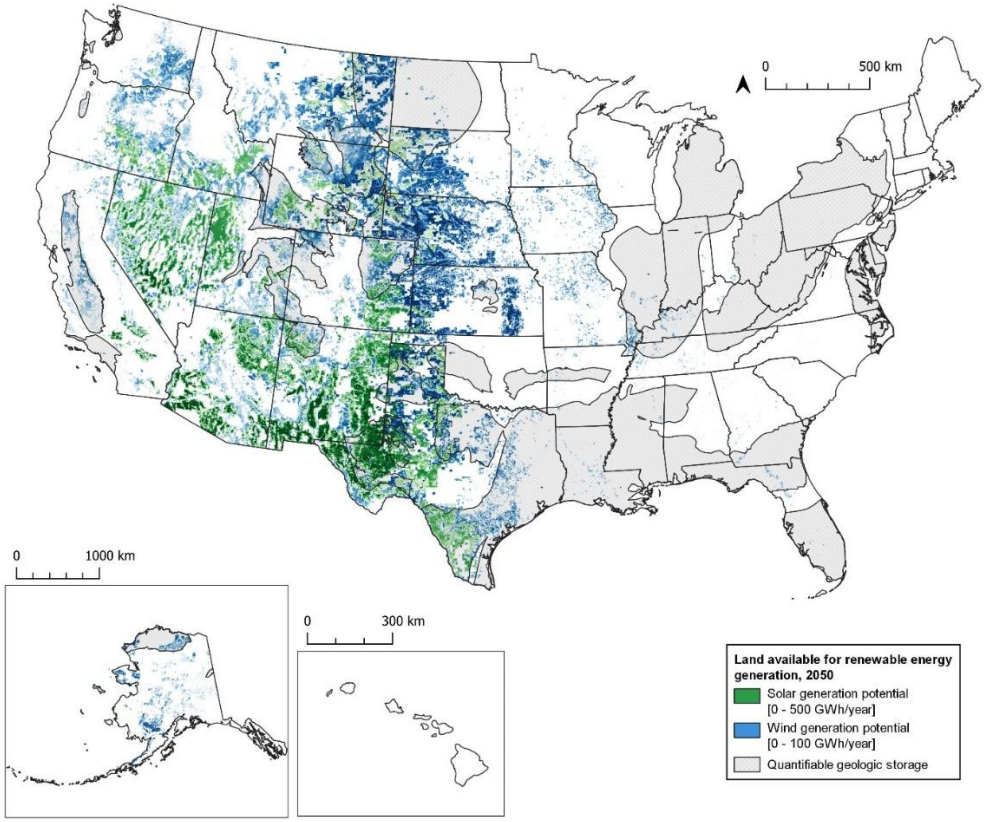

Figure 4. Identified suitable land for renewable energy generation for adsorbent DACS facilities in 2050, and their overlap with quantifiable geologic storage. Solar (green) and wind (blue) installations are color graded based on their generation potential, with darker colors indicating higher potential.

3.2.3. Impact of local climate on performance

Based on the impact of temperature and humidity on amine efficiency [52] and regeneration efficiency [53], DACS facilities deployed in colder drier regions were found to have increased capture productivity [31], such as those in the northwestern United States (**Figure S7**). Alaska, while having the lowest average yearly temperature in the United States, has low absolute levels of humidity (**Figure S8)** and thus cannot leverage the benefits of water vapor during the capture process.

3.2.4. Cost and technical potential for adsorbent DACS in 2050

First-of-a-kind total adsorbent DACS capacity was estimated at 41 kilotonnes of CO_2 per year between existing and planned operations by Climeworks [35,36] and Global Thermostat [37]. The modular nature of the adsorbent contactor means that, although these facilities may be considered pre-commercial-scale, the size of the core technology unit will not be subject to scaling. A blend of component-specific learning rates were considered for the pieces of equipment comprising adsorbent DACS [54–58]. Components with high degrees of modularity, or that are based on emerging science and technology such as the contactor and adsorbent media, were generally assigned higher learning rates [26,57], which are reflected in the reductions in cost between 2025 and 2050 (**Figure 5**). A recent study by Sievert et al. [59] used a similar methodology for an adsorbent DACS process, assigning learning rates ranging from 3-27% based on the novelty of the component [59]. Using

moderate rates for all components (**Table 1**) resulted in an overall learning rate of 9.7%, relatively conservative compared to other studies [26,59,60]. In addition to learning rates on capital expenditures, we applied learning to the thermal-energy requirement, fit to a target value at the final projected deployment in 2050. Our moderate estimate for thermal energy requirement was 7.6 GJ per tonne of CO_2, higher than several short- and long-term estimates [16,54] but lower than experimentally determined requirements at lab-scale [61,62]. The post-learning electricity requirement for adsorbent DACS, including generation of thermal energy via heat pump with a coefficient of performance of 2.5 (**Table S1**), was determined to be approximately 5.2 GJ per tonne of CO_2, and accounted for almost 20% of the post-learning cost reduction. The calculated energy requirement is similar to publicly reported estimates of energy requirements for current DAC plants by Carbon Engineering and Climeworks [25], and on the more conservative end of estimates for long-term capture facilities [16,26,54]. The contactor used for adsorption and regeneration is modular and was assumed to not benefit from economies of scale.

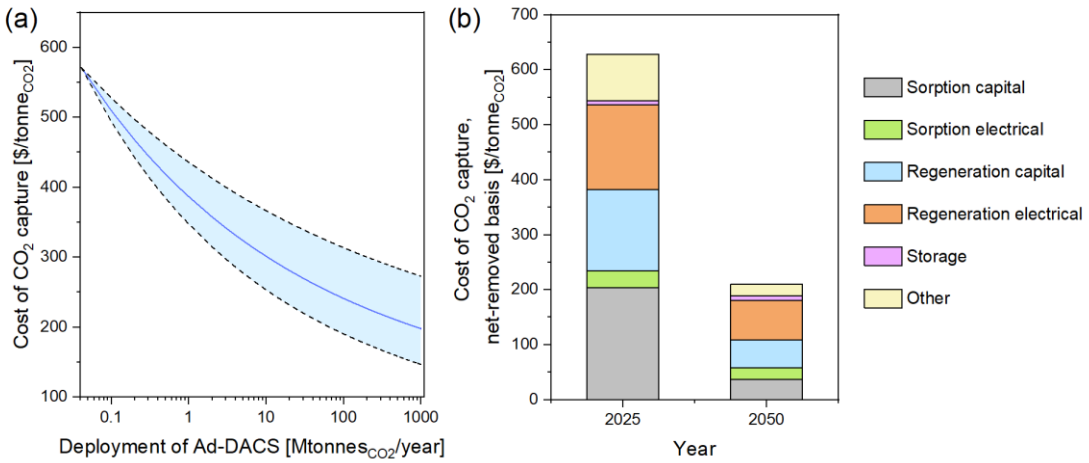

Figure 5. (a) Learning curves for adsorbent DACS for deployment up to 1 gigatonne of CO_2 per year, dark blue line indicates 'moderate' learning rate; (b) Cost breakdown of FOAK adsorbent DACS in 2025 and post-moderate learning adsorbent DACS located in in 2050. Both facilities

were assumed to operate at a scale of 0.3 megatonnes of CO_2 per year, at a location with identical climate, and utilize renewable electricity for energy supply.

Table 1. Component-based learning rates for adsorbent DAC technology learning.

Component	Learning rates	Moderate value
Adsorbent and contactor	10–15%	12%
Heat pump	5–12%	10%
Fans	2.5–7.5%	5%
Vacuum pumps	0–2.5%	0%
Drying and compression	0–2.5%	0%

Based on the quantity of renewable energy generation co-located with storage we estimate that, by 2050, approximately 2.5 and 6.8 gigatonnes of CO_2 per year could be captured utilizing adsorbent DACS powered by purpose-built wind and solar energy respectively. This value accounts for seasonal variations in CO_2 capture productivity, and learning-based improvements to the energy efficiency of the capture and regeneration process. While most regions in the United States have some potential to accommodate adsorbent DACS facilities, the largest opportunities for deployment are concentrated in: San Juan, McKinley, and Webb county, New Mexico; Reeves, Webb and Culberson county, Texas; North Slope, Alaska; Sweetwater and Carbon county, Wyoming. Capture costs vary from \$190–490 per tonne of CO_2, with a weighted average of \$250 per tonne of CO_2. Adsorbent DACS cost was primarily influenced by the scale of the facility and state-level electricity price, while local temperature and humidity had more minor impacts, matching the trends observed in the regional analysis by Terlouw et al. [27]. The states with the lowest DACS costs are generally expected to have the lowest costs for producing electricity and geologic storage, particularly Texas, New Mexico, and Wyoming. Several of these states were considered relatively undesirable in the near term for adsorbent DACS deployment based on

Figure 2, due to their carbon intensive electrical grid. However, the analysis for 2050 emphasizes the importance of decarbonization and its ability to significantly expand the potential for adsorbent DACS in pathways towards net-zero.

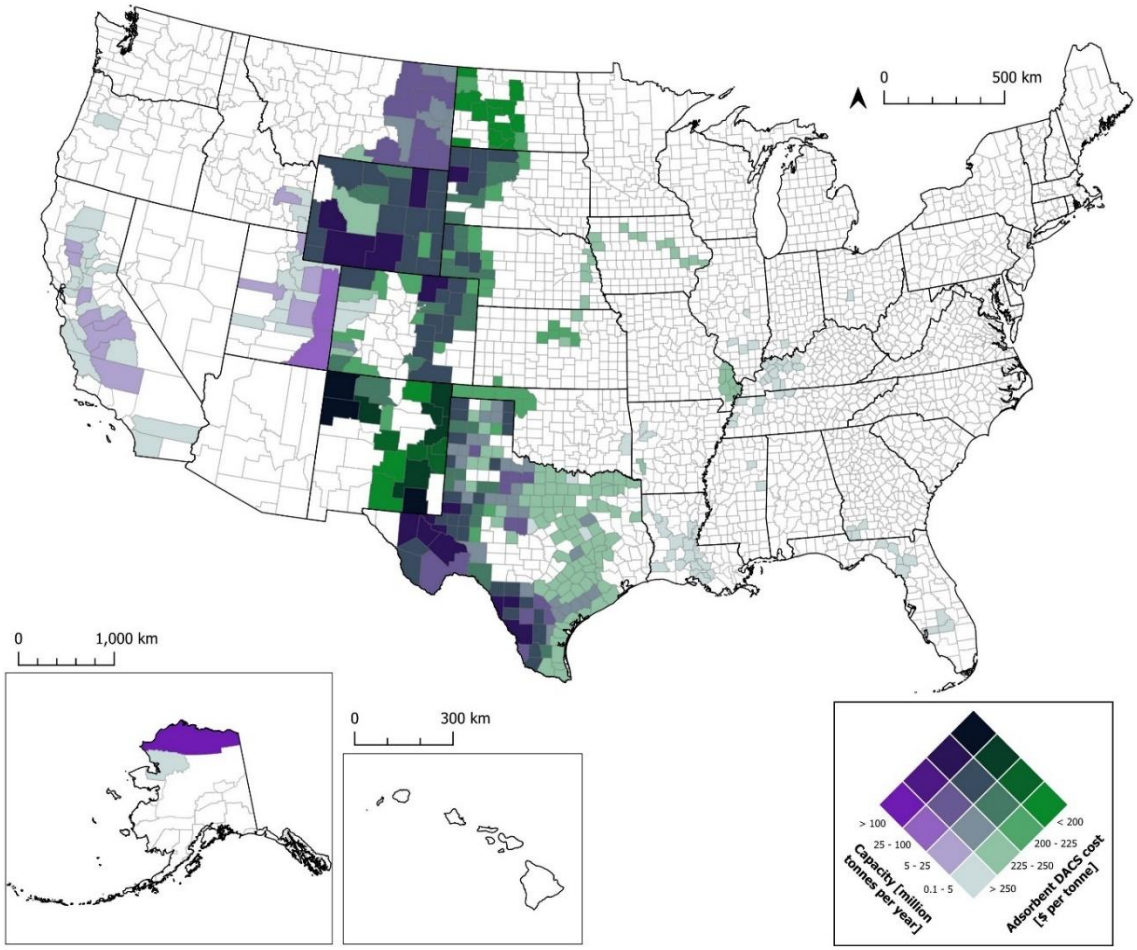

Figure 6. County-level assessment of potential cost and capacity of adsorbent DACS powered by renewable electricity, co-located with geologic storage.

3.4. Limitations of this study

The analysis in this work is intended to provide insight into the deployment of adsorbent-based direct air capture and storage in the United States, both in the near- and long-term as we move towards net-zero emissions. To carry out this analysis a number of assumptions were made, and

several aspects of DACS deployment were outside the scope of this study and should be addressed in future work.

While the assumptions for siting of renewable energy generation and DACS facilities were relatively restrictive, this work did not account for state- or county-level restrictions and ordinances [63]. The potential overlap in lands utilized for direct air capture and other carbon removal technologies, such as biomass carbon removal and storage (BiCRS) or forest management, was not quantified in this work, but can be found elsewhere [2,64].

The carbon intensity of energy generation, and by extension CO_2 capture, is quantified in this work; however, the broader environmental impact and burdens of these facilities were not. For example large-scale deployment of direct air capture would require concurrent scale-up of supply chains for raw materials related to the capture media [65], such as reagents for the synthesis of amine-rich polymers [25]. To understand these impacts on cost and viability, full life-cycle assessment (LCA) of the capture facility is required, and will be dependent on the specific technology, the scale of the facility, and its location.

Quantifiable geologic storage was an essential part of this analysis, providing a durable method of sequestering captured CO_2. The utilization of pipelines to transport CO_2 to suitable geologic storage was also not investigated in this work as, due to uncertainties around public perception [66] and their location depending on the location of CO_2 sources and sinks, predicting their long-term deployment is challenging. Other analyses, such as the 'Roads to Removal' [2] and 'Net Zero America' [67] have conducted assessments of CO_2 pipeline infrastructure and its role in achieving net-zero emissions by 2050. There are also analyses of other transport options such as road, rail, and barge, the costs for which vary strongly by the quantity and travel distance of CO_2 being transported [68–70].

3.5. Outlook for adsorbent DACS deployment in the continental United States

These analyses provide a foundation for further study on direct air capture and storage across the global, not only within the United States. Challenges with heat supply and the current carbon intensity of the United States' electrical grid further support the need for prioritizing grid decarbonization, not only to reduce emissions but improve the efficiency of capture processes utilizing electrified processes. In the near-term, the viability of grid electricity for powering DACS is strongly dependent on location, due to the energy mix and carbon intensity of each state's electrical grid. States like Vermont and Washington have relatively low capture costs in the near-term due to their high proportion of renewables, resulting in net-removed capture efficiencies of 99 and 81% respectively, but geologic storage availability makes these locations challenging in absence of robust and inexpensive CO_2 transportation networks. On the other hand, states with ample geologic storage resources have much lower capture efficiencies, with Texas having only 19% and Wyoming's carbon intensive grid resulting in DACS being a net producer of CO_2.

After applying moderate component learning rates to the DACS process, we estimate that 9.3 gigatonnes of CO_2 could be captured utilizing purpose-built renewable energy by 2050. Much of this capacity is concentrated in several states (Texas, Wyoming, New Mexico, California, and Alaska) due to a combination of land availability and suitable weather for electricity generation. An average capture cost of $250 per tonne was calculated, with regions such as Texas, Wyoming and New Mexico having substantially lower costs due to the scale of facilities possible, and their low electricity and storage costs. The high-resolution geospatial analysis emphasizes the need for region-specific research, as local environment and terrain are likely to have a strong impact on both the performance of a capture facility, and the cost for constructing and operating one.

However, this work identifies a number of high potential regions for long-term DACS deployment at a gigatonne scale, which could cement its role in a pathway towards net-zero.

ASSOCIATED CONTENT

Supporting Information. Information related to the process model, cost and capacity calculations, and methodology for adsorbent DACS deployment in the short- and long-term; results and discussion pertaining to adsorbent DACS paired with geothermal heat.

AUTHOR INFORMATION

Corresponding Author

* cdscown@lbl.gov

** pang6@llnl.gov

Author Contributions

The manuscript was written through contributions of all authors. All authors have given approval to the final version of the manuscript.

‡ These authors contributed equally.

ACKNOWLEDGMENT

Funding for this research was provided by the U.S. Department of Energy (DOE) Office of Fossil Energy and Carbon Management (FECM) and Office of Energy Efficiency and Renewable Energy Bioenergy Technologies Office (BETO). This work was also part of the Joint BioEnergy Institute (https://www.jbei.org) supported by the U.S. DOE, Office of Science, Office of Biological and

Environmental Research. Additional funds were contributed by the ClimateWorks Foundation. We thank Jennifer Pett-Ridge, Roger Aines, Sarah Baker, Sara Kuebbing, Allegra Mayer, Kimberley Mayfield, Peter Psarras, and Drew Wong for helpful discussions and gratefully thank Jeannette Yusko and Janelle Cataldo for graphic support. The views expressed in the article do not necessarily represent the views of the DOE or the U.S. Government. Work conducted at Lawrence Livermore National Laboratory (LLNL) was supported under the auspices of the U.S. Department of Energy (DOE) under Contract DE-AC52-07NA27344 and at Lawrence Berkeley National Laboratory through Contract DE-AC02-05CH11231. The United States Government retains and the publisher, by accepting the article for publication, acknowledges that the United States Government retains a nonexclusive, paid-up, irrevocable, worldwide license to publish or reproduce the published form of this manuscript or allow others to do so, for United States Government purposes.

ABBREVIATIONS

BECCS, Bioenergy with carbon capture and storage; BiCRS, Biomass carbon removal and storage; CDR, carbon dioxide removal; CO_2, carbon dioxide; DAC, direct air capture; DACS, direct air capture and storage; FOAK, first-of-a-kind; GAP, Gap Analysis Project; NLCD, National Land Cover Database; NREL, National Renewable Energy Laboratory

REFERENCES

(1) Committee on Developing a Research Agenda for Carbon Dioxide Removal and Reliable Sequestration; Board on Atmospheric Sciences and Climate; Board on Energy and Environmental Systems; Board on Agriculture and Natural Resources; Board on Earth Sciences and Resources; Board on Chemical Sciences and Technology; Ocean Studies Board; Division on Earth and Life Studies; National Academies of Sciences, Engineering, and Medicine. *Negative Emissions Technologies and Reliable Sequestration: A Research Agenda*; National Academies Press: Washington, D.C., 2019; p 25259. https://doi.org/10.17226/25259.

(2) Pett-Ridge, J.; Ammar, H. Z.; Aui, A.; Ashton, M.; Baker, S. E.; Basso, B.; Bradford, M.; Bump, A. P.; Busch, I.; Calzado, E. R.; Chirigotis, J. W.; Clauser, N.; Crotty, S.; Dahl, N.; Dai, T.; Ducey, M.; Dumortier, J.; Ellebracht, N. C.; Egui, R. G.; Fowler, A.; Georgiou, K.; Giannopoulos, D.; Goldstein, H.; Harris, T.; Hayes, D.; Hellwinckel, C.; Ho, A.; Hong, M.; Hovorka, S.; Hunter-Sellars, E.; Kirkendall, W.; Kuebbing, S.; Langholtz, M.; Layer, M.; Lee, I.; Lewis, R.; Li, W.; Liu, W.; Lozano, J. T.; Lunstrum, A.; Mayer, A. C.; Mayfield, K. K.; McNeil, W.; Nico, P.; O'Rourke, A.; Pang, S. H.; Paustian, K.; Peridas, G.; Pilorge, H.; Pisciotta, M.; Price, L.; Psarras, P.; Robertson, G. P.; Sagues, W. J.; Sanchez, D. L.; Scown, C. D.; Schmidt, B. M.; Slessarev, E. W.; Sokol, N.; Stanley, A. J.; Swan, A.; Toureene, C.; Wong, A. A.; Wright, M. M.; Yao, Y.; Zhang, B.; Zhang, Y.; Aines, R. D. *Roads to Removal: Options for Carbon Dioxide Removal in the United States*; LLNL-TR-852901; Lawrence Livermore National Laboratory: Lawrence Livermore National Laboratory, 2023. https://doi.org/10.2172/2301853.

(3) Smith, P.; Davis, S. J.; Creutzig, F.; Fuss, S.; Minx, J.; Gabrielle, B.; Kato, E.; Jackson, R. B.; Cowie, A.; Kriegler, E.; Van Vuuren, D. P.; Rogelj, J.; Ciais, P.; Milne, J.; Canadell, J. G.; McCollum, D.; Peters, G.; Andrew, R.; Krey, V.; Shrestha, G.; Friedlingstein, P.; Gasser, T.; Grübler, A.; Heidug, W. K.; Jonas, M.; Jones, C. D.; Kraxner, F.; Littleton, E.; Lowe, J.; Moreira, J. R.; Nakicenovic, N.; Obersteiner, M.; Patwardhan, A.; Rogner, M.; Rubin, E.; Sharifi, A.; Torvanger, A.; Yamagata, Y.; Edmonds, J.; Yongsung, C. Biophysical and Economic Limits to Negative CO2 Emissions. *Nature Clim Change* **2016**, *6* (1), 42–50. https://doi.org/10.1038/nclimate2870.

(4) Baker, S. E.; Stolaroff, J. K.; Peridas, G.; Pang, S. H.; Goldstein, H. M.; Lucci, F. R.; Li, W.; Slessarev, E. W.; Pett-Ridge, J.; Ryerson, F. J.; Wagoner, J. L.; Kirkendall, W.; Aines, R. D.; Sanchez, D. L.; Cabiyo, B.; Baker, J.; McCoy, S.; Uden, S.; Runnebaum, R.; Wilcox, J.; Psarras, P. C.; Pilorgé, H.; McQueen, N.; Maynard, D.; McCormick, C. *Getting to Neutral: Options for Negative Carbon Emissions in California*; LLNL-TR-796100; Lawrence Livermore National Laboratory: Lawrence Livermore National Laboratory, 2020. https://doi.org/10.2172/1597217.

(5) Sanz-Pérez, E. S.; Murdock, C. R.; Didas, S. A.; Jones, C. W. Direct Capture of CO2 from Ambient Air. *Chem. Rev.* **2016**, *116* (19), 11840–11876. https://doi.org/10.1021/acs.chemrev.6b00173.

(6) Keith, D. W.; Holmes, G.; St. Angelo, D.; Heidel, K. A Process for Capturing CO2 from the Atmosphere. *Joule* **2018**, *2* (8), 1573–1594. https://doi.org/10.1016/j.joule.2018.05.006.

(7) McQueen, N.; Desmond, M. J.; Socolow, R. H.; Psarras, P.; Wilcox, J. Natural Gas vs. Electricity for Solvent-Based Direct Air Capture. *Front. Clim.* **2021**, *2*, 618644. https://doi.org/10.3389/fclim.2020.618644.

(8) Beuttler, C.; Charles, L.; Wurzbacher, J. The Role of Direct Air Capture in Mitigation of Anthropogenic Greenhouse Gas Emissions. *Front. Clim.* **2019**, *1*, 10. https://doi.org/10.3389/fclim.2019.00010.

(9) Gadikota, G. Carbon Mineralization Pathways for Carbon Capture, Storage and Utilization. *Commun Chem* **2021**, *4* (1), 23. https://doi.org/10.1038/s42004-021-00461-x.

(10) McQueen, N.; Kelemen, P.; Dipple, G.; Renforth, P.; Wilcox, J. Ambient Weathering of Magnesium Oxide for CO2 Removal from Air. *Nat Commun* **2020**, *11* (1), 3299. https://doi.org/10.1038/s41467-020-16510-3.

(11) Fu, D.; Park, Y.; Davis, M. E. Confinement Effects Facilitate Low-Concentration Carbon Dioxide Capture with Zeolites. *Proc. Natl. Acad. Sci. U.S.A.* **2022**, *119* (39), e2211544119. https://doi.org/10.1073/pnas.2211544119.

(12) Wang, T.; Lackner, K. S.; Wright, A. Moisture Swing Sorbent for Carbon Dioxide Capture from Ambient Air. *Environ. Sci. Technol.* **2011**, *45* (15), 6670–6675. https://doi.org/10.1021/es201180v.

(13) Digdaya, I. A.; Sullivan, I.; Lin, M.; Han, L.; Cheng, W.-H.; Atwater, H. A.; Xiang, C. A Direct Coupled Electrochemical System for Capture and Conversion of CO2 from Oceanwater. *Nat Commun* **2020**, *11* (1), 4412. https://doi.org/10.1038/s41467-020-18232-y.

(14) Li, X.; Zhao, X.; Liu, Y.; Hatton, T. A.; Liu, Y. Redox-Tunable Lewis Bases for Electrochemical Carbon Dioxide Capture. *Nat Energy* **2022**, *7* (11), 1065–1075. https://doi.org/10.1038/s41560-022-01137-z.
(15) Lebling, K.; Leslie-Bole, H.; Byrum, Z.; Bridgwater, E. 6 Things to Know About Direct Air Capture. *World Resources Institute*. May 2, 2022. https://www.wri.org/insights/direct-air-capture-resource-considerations-and-costs-carbon-removal.
(16) McQueen, N.; Psarras, P.; Pilorgé, H.; Liguori, S.; He, J.; Yuan, M.; Woodall, C. M.; Kian, K.; Pierpoint, L.; Jurewicz, J.; Lucas, J. M.; Jacobson, R.; Deich, N.; Wilcox, J. Cost Analysis of Direct Air Capture and Sequestration Coupled to Low-Carbon Thermal Energy in the United States. *Environ. Sci. Technol.* **2020**, *54* (12), 7542–7551. https://doi.org/10.1021/acs.est.0c00476.
(17) Terlouw, T.; Treyer, K.; Bauer, C.; Mazzotti, M. Life Cycle Assessment of Direct Air Carbon Capture and Storage with Low-Carbon Energy Sources. *Environ. Sci. Technol.* **2021**, *55* (16), 11397–11411. https://doi.org/10.1021/acs.est.1c03263.
(18) Sadiq, M. M.; Batten, M. P.; Mulet, X.; Freeman, C.; Konstas, K.; Mardel, J. I.; Tanner, J.; Ng, D.; Wang, X.; Howard, S.; Hill, M. R.; Thornton, A. W. A Pilot-Scale Demonstration of Mobile Direct Air Capture Using Metal-Organic Frameworks. *Adv. Sustainable Syst.* **2020**, *4* (12), 2000101. https://doi.org/10.1002/adsu.202000101.
(19) *Noya: Our Approach*. https://www.noya.co/how-it-works (accessed 2024-02-15).
(20) Lebling, K.; Leslie-Bole, H.; Psarras, P.; Bridgwater, E.; Byrum, Z.; Pilorgé, H. Direct Air Capture: Assessing Impacts to Enable Responsible Scaling. *WRIPUB* **2022**. https://doi.org/10.46830/wriwp.21.00058.
(21) Viebahn, P.; Scholz, A.; Zelt, O. The Potential Role of Direct Air Capture in the German Energy Research Program—Results of a Multi-Dimensional Analysis. *Energies* **2019**, *12* (18), 3443. https://doi.org/10.3390/en12183443.
(22) U.S. Geological Survey Geologic Carbon Dioxide Storage Resources Assessment Team. *National Assessment of Geologic Carbon Dioxide Storage Resources- Summary*; Fact Sheet; U.S. Geological Survey Fact Sheet 2013–3020; 2013. https://pubs.usgs.gov/fs/2013/3020/.
(23) Pilorgé, H.; Kolosz, B.; Wu, G. C.; Wilcox, J.; Freedman, J. *Global Mapping of CDR Opportunities*. CDR Primer. https://cdrprimer.org/ (accessed 2024-02-05).
(24) Nemet, G. F.; Gidden, M. J.; Greene, J.; Roberts, C.; Lamb, W. F.; Minx, J. C.; Smith, S. M.; Geden, O.; Riahi, K. Near-Term Deployment of Novel Carbon Removal to Facilitate Longer-Term Deployment. *Joule* **2023**, *7* (12), 2653–2659. https://doi.org/10.1016/j.joule.2023.11.001.
(25) McQueen, N.; Gomes, K. V.; McCormick, C.; Blumanthal, K.; Pisciotta, M.; Wilcox, J. A Review of Direct Air Capture (DAC): Scaling up Commercial Technologies and Innovating for the Future. *Prog. Energy* **2021**, *3* (3), 032001. https://doi.org/10.1088/2516-1083/abf1ce.
(26) Young, J.; McQueen, N.; Charalambous, C.; Foteinis, S.; Hawrot, O.; Ojeda, M.; Pilorgé, H.; Andresen, J.; Psarras, P.; Renforth, P.; Garcia, S.; Van Der Spek, M. The Cost of Direct Air Capture and Storage Can Be Reduced via Strategic Deployment but Is Unlikely to Fall below Stated Cost Targets. *One Earth* **2023**, *6* (7), 899–917. https://doi.org/10.1016/j.oneear.2023.06.004.
(27) Terlouw, T.; Pokras, D.; Becattini, V.; Mazzotti, M. Assessment of Potential and Techno-Economic Performance of Solid Sorbent Direct Air Capture with CO_2 Storage in Europe. *Environ. Sci. Technol.* **2024**, *58* (24), 10567–10581. https://doi.org/10.1021/acs.est.3c10041.
(28) International Energy Agency. *Direct Air Capture: A Key Technology for Net Zero*; OECD, 2022. https://doi.org/10.1787/bbd20707-en.
(29) Fauvel, C.; Fuhrman, J.; Ou, Y.; Shobe, W.; Doney, S.; McJeon, H.; Clarens, A. Regional Implications of Carbon Dioxide Removal in Meeting Net Zero Targets for the United States. *Environ. Res. Lett.* **2023**, *18* (9), 094019. https://doi.org/10.1088/1748-9326/aced18.
(30) Fahr, S.; Powell, J.; Favero, A.; Giarrusso, A. J.; Lively, R. P.; Realff, M. J. Assessing the Physical Potential Capacity of Direct Air Capture with Integrated Supply of Low-carbon Energy Sources. *Greenhouse Gases* **2022**, *12* (1), 170–188. https://doi.org/10.1002/ghg.2136.

(31) Sendi, M.; Bui, M.; Mac Dowell, N.; Fennell, P. Geospatial Analysis of Regional Climate Impacts to Accelerate Cost-Efficient Direct Air Capture Deployment. *One Earth* **2022**, *5* (10), 1153–1164. https://doi.org/10.1016/j.oneear.2022.09.003.
(32) Heydari-Gorji, A.; Sayari, A. Thermal, Oxidative, and CO_2-Induced Degradation of Supported Polyethylenimine Adsorbents. *Ind. Eng. Chem. Res.* **2012**, *51* (19), 6887–6894. https://doi.org/10.1021/ie3003446.
(33) U.S. Energy Information Administration (EIA). EIA-861 Annual Electric Power Industry Report: Annual Sales to Ultimate Customers by State and Sector (2010-2022), 2023. https://www.eia.gov/electricity/data/state/.
(34) U.S. Energy Information Administration (EIA). State Electricity Profiles (2021), 2022. https://www.eia.gov/electricity/state/archive/2021/.
(35) Climeworks. *Orca: the first large-scale plant*. https://climeworks.com/plant-orca (accessed 2024-04-26).
(36) Climeworks. *Mammoth: our newest facility*. https://climeworks.com/plant-mammoth (accessed 2024-04-26).
(37) Global Thermostat. *Global Thermostat unveils one of the world's largest units for removing carbon dioxide directly from the air*. https://www.globalthermostat.com/news-and-updates/global-thermostat-colorado-headquarters (accessed 2024-04-26).
(38) Gagnon, P.; Cowiestoll, B.; Schwarz, M. *Cambium 2022 Scenario Descriptions and Documentation*; NREL/TP-6A40-84916; National Renewable Energy Laboratory, 2023. https://www.nrel.gov/research/publications.
(39) National Renewable Energy Laboratory. *Annual Technology Baseline*. https://atb.nrel.gov/ (accessed 2024-02-20).
(40) Dewitz, J.; U.S. Geological Survey. National Land Cover Database (NLCD) 2019 Products (Ver. 2.0), 2021. https://doi.org/10.5066/P9KZCM54.
(41) Denholm, P.; Brown, P.; Cole, W.; Mai, T.; Sergi, B.; Brown, M.; Jadun, P.; Ho, J.; Mayernik, J.; McMillan, C.; Sreenath, R. *Examining Supply-Side Options to Achieve 100% Clean Electricity by 2035*; NREL/TP-6A40-81644, 1885591, MainId:82417; 2022; p NREL/TP-6A40-81644, 1885591, MainId:82417. https://doi.org/10.2172/1885591.
(42) U.S. Energy Information Administration (EIA). *Annual Energy Outlook 2022: Narrative*; AEO2022 Narrative; 2022. https://www.eia.gov/outlooks/aeo/electricity_generation.php.
(43) Golubkova, K.; Kim, C.-R.; Paul, S. Japan Sees Need for Sharp Hike in Power Output by 2050 to Meet Demand from AI, Chip Plants. *Reuters*. May 13, 2024. https://www.reuters.com/business/energy/japan-sees-need-sharp-hike-power-output-by-2050-meet-demand-ai-chip-plants-2024-05-14/.
(44) Schwabe, P. *Solar Energy Prospecting in Remote Alaska: An Economic Analysis of Solar Photovoltaics in the Last Frontier State*; NREL/TP--6A20-65834, DOE/IE--0040, 1239239; 2016; p NREL/TP--6A20-65834, DOE/IE--0040, 1239239. https://doi.org/10.2172/1239239.
(45) Harrison-Atlas, D.; Lopez, A.; Lantz, E. Dynamic Land Use Implications of Rapidly Expanding and Evolving Wind Power Deployment. *Environ. Res. Lett.* **2022**, *17* (4), 044064. https://doi.org/10.1088/1748-9326/ac5f2c.
(46) Bolinger, M.; Bolinger, G. Land Requirements for Utility-Scale PV: An Empirical Update on Power and Energy Density. *IEEE Journal of Photovoltaics* **2022**, *12* (2), 589–594. https://doi.org/10.1109/JPHOTOV.2021.3136805.
(47) Ho, A.; Giannopoulos, D.; Pilorgé, H.; Psarras, P. Opportunities for Rail in the Transport of Carbon Dioxide in the United States. *Front. Energy Res.* **2024**, *11*, 1343085. https://doi.org/10.3389/fenrg.2023.1343085.
(48) NASA Center For Climate Simulation. NASA Earth Exchange Global Daily Downscaled Projections (NEX-GDDP-CMIP6), 2021. https://doi.org/10.7917/OFSG3345.

(49) Sendi, M.; Bui, M.; Mac Dowell, N.; Fennell, P. Geospatial Techno-Economic and Environmental Assessment of Different Energy Options for Solid Sorbent Direct Air Capture. *Cell Reports Sustainability* **2024**, *1* (8). https://doi.org/10.1016/j.crsus.2024.100151.
(50) Lopez, A.; Mai, T.; Lantz, E.; Harrison-Atlas, D.; Williams, T.; Maclaurin, G. Land Use and Turbine Technology Influences on Wind Potential in the United States. *Energy* **2021**, *223*, 120044. https://doi.org/10.1016/j.energy.2021.120044.
(51) Omitaomu, O. A.; Blevins, B. R.; Jochem, W. C.; Mays, G. T.; Belles, R.; Hadley, S. W.; Harrison, T. J.; Bhaduri, B. L.; Neish, B. S.; Rose, A. N. Adapting a GIS-Based Multicriteria Decision Analysis Approach for Evaluating New Power Generating Sites. *Applied Energy* **2012**, *96*, 292–301. https://doi.org/10.1016/j.apenergy.2011.11.087.
(52) Said, R. B.; Kolle, J. M.; Essalah, K.; Tangour, B.; Sayari, A. A Unified Approach to CO_2 –Amine Reaction Mechanisms. *ACS Omega* **2020**, *5* (40), 26125–26133. https://doi.org/10.1021/acsomega.0c03727.
(53) Wurzbacher, J. A.; Gebald, C.; Brunner, S.; Steinfeld, A. Heat and Mass Transfer of Temperature–Vacuum Swing Desorption for CO2 Capture from Air. *Chemical Engineering Journal* **2016**, *283*, 1329–1338. https://doi.org/10.1016/j.cej.2015.08.035.
(54) Fasihi, M.; Efimova, O.; Breyer, C. Techno-Economic Assessment of CO2 Direct Air Capture Plants. *Journal of Cleaner Production* **2019**, *224*, 957–980. https://doi.org/10.1016/j.jclepro.2019.03.086.
(55) Deutz, S.; Bardow, A. Life-Cycle Assessment of an Industrial Direct Air Capture Process Based on Temperature–Vacuum Swing Adsorption. *Nat Energy* **2021**, *6* (2), 203–213. https://doi.org/10.1038/s41560-020-00771-9.
(56) Yeh, S.; Rubin, E. S. A Review of Uncertainties in Technology Experience Curves. *Energy Economics* **2012**, *34* (3), 762–771. https://doi.org/10.1016/j.eneco.2011.11.006.
(57) Malhotra, A.; Schmidt, T. S. Accelerating Low-Carbon Innovation. *Joule* **2020**, *4* (11), 2259–2267. https://doi.org/10.1016/j.joule.2020.09.004.
(58) Riahi, K.; Rubin, E. S.; Taylor, M. R.; Schrattenholzer, L.; Hounshell, D. Technological Learning for Carbon Capture and Sequestration Technologies. *Energy Economics* **2004**, *26* (4), 539–564. https://doi.org/10.1016/j.eneco.2004.04.024.
(59) Sievert, K.; Schmidt, T. S.; Steffen, B. Considering Technology Characteristics to Project Future Costs of Direct Air Capture. *Joule* **2024**, *8* (4), 979–999. https://doi.org/10.1016/j.joule.2024.02.005.
(60) Lackner, K. S.; Azarabadi, H. Buying down the Cost of Direct Air Capture. *Ind. Eng. Chem. Res.* **2021**, *60* (22), 8196–8208. https://doi.org/10.1021/acs.iecr.0c04839.
(61) Luukkonen, A.; Elfving, J.; Inkeri, E. Improving Adsorption-Based Direct Air Capture Performance through Operating Parameter Optimization. *Chemical Engineering Journal* **2023**, *471*, 144525. https://doi.org/10.1016/j.cej.2023.144525.
(62) Bos, M. J.; Pietersen, S.; Brilman, D. W. F. Production of High Purity CO2 from Air Using Solid Amine Sorbents. *Chemical Engineering Science: X* **2019**, *2*, 100020. https://doi.org/10.1016/j.cesx.2019.100020.
(63) Lopez, A.; Cole, W.; Sergi, B.; Levine, A.; Carey, J.; Mangan, C.; Mai, T.; Williams, T.; Pinchuk, P.; Gu, J. Impact of Siting Ordinances on Land Availability for Wind and Solar Development. *Nat Energy* **2023**, *8* (9), 1034–1043. https://doi.org/10.1038/s41560-023-01319-3.
(64) Dai, T.; Ellebracht, N. C.; Hunter-Sellars, E.; Aui, A.; Goldstein, H. M.; Li, W.; Hellwinckel, C.; Price, L.; Wong, A. A.; Nico, P.; Basso, B.; Roberton, P. G.; Pett-Ridge, J.; Langholtz, M.; Baker, S. E.; Pang, S. H.; Scown, C. D. Land Resources and the Implications for Scaling Engineered Carbon Dioxide Removal in the United States. *Energy & Environmental Science (Submitted, EE-ANA-10-2024-004788)*.
(65) Qiu, Y.; Lamers, P.; Daioglou, V.; McQueen, N.; de Boer, H.-S.; Harmsen, M.; Wilcox, J.; Bardow, A.; Suh, S. Environmental Trade-Offs of Direct Air Capture Technologies in Climate Change

Mitigation toward 2100. *Nat Commun* **2022**, *13* (1), 3635. https://doi.org/10.1038/s41467-022-31146-1.
(66) Gough, C.; O'Keefe, L.; Mander, S. Public Perceptions of CO2 Transportation in Pipelines. *Energy Policy* **2014**, *70*, 106–114. https://doi.org/10.1016/j.enpol.2014.03.039.
(67) Jenkins, J. D.; Mayfield, E. N.; Larson, E. D.; Pacala, S. W.; Greig, C. Mission Net-Zero America: The Nation-Building Path to a Prosperous, Net-Zero Emissions Economy. *Joule* **2021**, *5* (11), 2755–2761. https://doi.org/10.1016/j.joule.2021.10.016.
(68) Oeuvray, P.; Burger, J.; Roussanaly, S.; Mazzotti, M.; Becattini, V. Multi-Criteria Assessment of Inland and Offshore Carbon Dioxide Transport Options. *Journal of Cleaner Production* **2024**, *443*, 140781. https://doi.org/10.1016/j.jclepro.2024.140781.
(69) Stolaroff, J. K.; Pang, S. H.; Li, W.; Kirkendall, W. G.; Goldstein, H. M.; Aines, R. D.; Baker, S. E. Transport Cost for Carbon Removal Projects With Biomass and CO2 Storage. *Front. Energy Res.* **2021**, *9*, 639943. https://doi.org/10.3389/fenrg.2021.639943.
(70) Myers, C.; Li, W.; Markham, G. The Cost of CO2 Transport by Truck and Rail in the United States. *International Journal of Greenhouse Gas Control* **2024**, *134*, 104123. https://doi.org/10.1016/j.ijggc.2024.104123.

SYNOPSIS

Current energy supplies for direct air capture significantly increase net-removed cost. High-resolution geospatial analysis is used to assess the deployment of renewable-powered direct air capture in the United States, quantifying capacity and cost at the county level.

The potential and cost of carbon dioxide removal using direct air capture with land-based wind and utility-scale photovoltaics

Supplementary Information

Elwin Hunter-Sellars,[a,‡] Tao Dai,[b,c,‡] Nathan C. Ellebracht,[a] Hélène Pilorgé,[d] Maxwell Pisciotta,[d] Alexander P. Bump,[e] Edna Rodriguez Calzado,[e] Susan D. Hovorka,[e] Corinne D. Scown,[b,c,f,g,] Simon H. Pang[a,**]*

[a] Materials Science Division, Lawrence Livermore National Laboratory, Livermore, CA, USA

[b] Biological Systems & Engineering Division, Lawrence Berkeley National Laboratory, Berkeley, CA, USA

[c] Joint BioEnergy Institute, Emeryville, CA, USA

[d] Department of Chemical and Biomolecular Engineering, University of Pennsylvania, Philadelphia, PA, USA

[e] Bureau of Economic Geology, The University of Texas at Austin, Austin, TX, USA

[f] Energy Analysis & Environmental Impacts Division, Lawrence Berkeley National Laboratory, Berkeley, CA, USA

[g] Energy & Biosciences Institute, University of California, Berkeley, Berkeley, CA, USA

[‡] these authors contributed equally to this work

Email: * cdscown@lbl.gov; ** pang6@llnl.gov

Table S1. Adsorbent DACS process information, including scale and cost parameters

Parameter	Units	Baseline value
Baseline adsorbent cyclic working capacity (30°C, 0% RH)	$mol_{CO2}/kg_{adsorbent}$	0.8
Mass ratio of contactor to adsorbent	$kg_{contactor}/kg_{adsorbent}$	0.2
Average CO_2 removal efficiency	%	75
Cycle time	mins	20
Degradation rate constant, k		5.1×10^{-5}
Relative CO_2 capture capacity prior to sorbent replacement	%	70
Adsorbent material lifetime [a]	years	0.3
Contactor lifetime	years	10
Contactor length	m	0.3
Contactor channel size	mm	0.5
Fan electricity requirement [1,2]	$GJ/tonne_{CO2}$	1.1
Vacuum pump electricity requirement [1]	$GJ/tonne_{CO2}$	0.6
Compressor electricity requirement [3]	$GJ/tonne_{CO2}$	0.3
Regeneration steam requirement [4]	$GJ/tonne_{CO2}$	12.1
Heat pump coefficient of performance [b]		2.5
Plant scale (low, nearby generation)	$tonneCO_2/y$	100,000
Plant scale (moderate, nearby generation)	$tonneCO_2/y$	300,000
Plant scale (high. nearby generation)	$tonneCO_2/y$	1,000,000
Capacity factor		0.9
Average storage cost	$\$/tonneCO_2$	7.75
Storage cost range	$\$/tonneCO_2$	3.95 - 135
Labor and maintenance	*% total OPEX*	4.5
Balance of plant CAPEX	*% total CAPEX*	10
Capital scaling factor	$\$_{overnight}/\$_{bare}$	4.5
Plant lifetime	*years*	20
Capital discount rate	*%*	12.5

[a] Adsorbent lifetime is a derived parameter based on the degradation rate constant, full cycle time, and relative capacity at the time of sorbent replacement. Residual capacity = $(1–k)^n$ where n is the number of cycles.

[b] Based on a heat pump system using recovered heat from excess steam, air, and/or low-grade process, waste, or renewable heat sources.

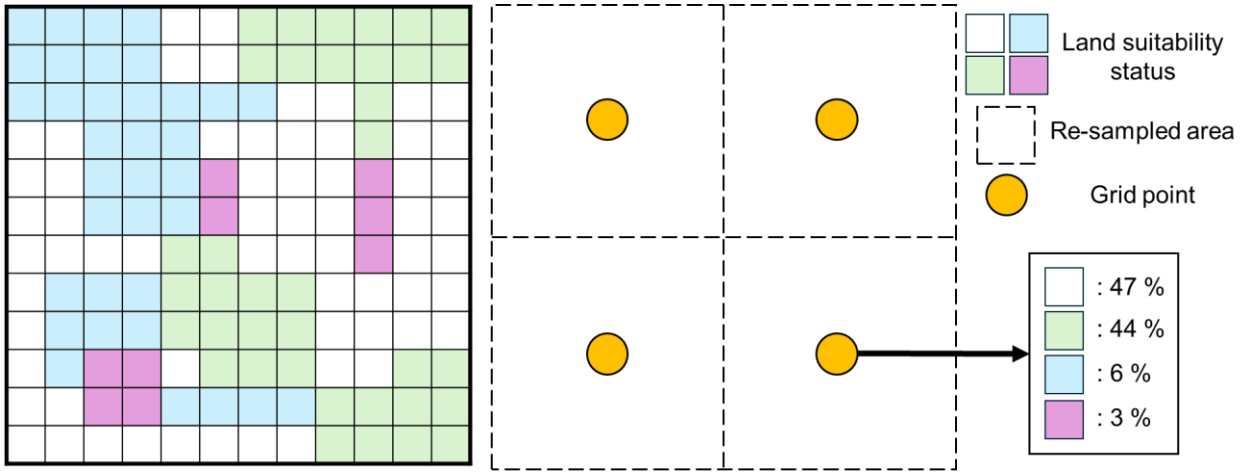

Figure S1. Schematic depicting the process of aggregating higher resolution dataset into lower resolution dataset with corresponding grid points. This resampling process retains the information of the fraction of suitable land contained within each re-sampled area within each grid point.

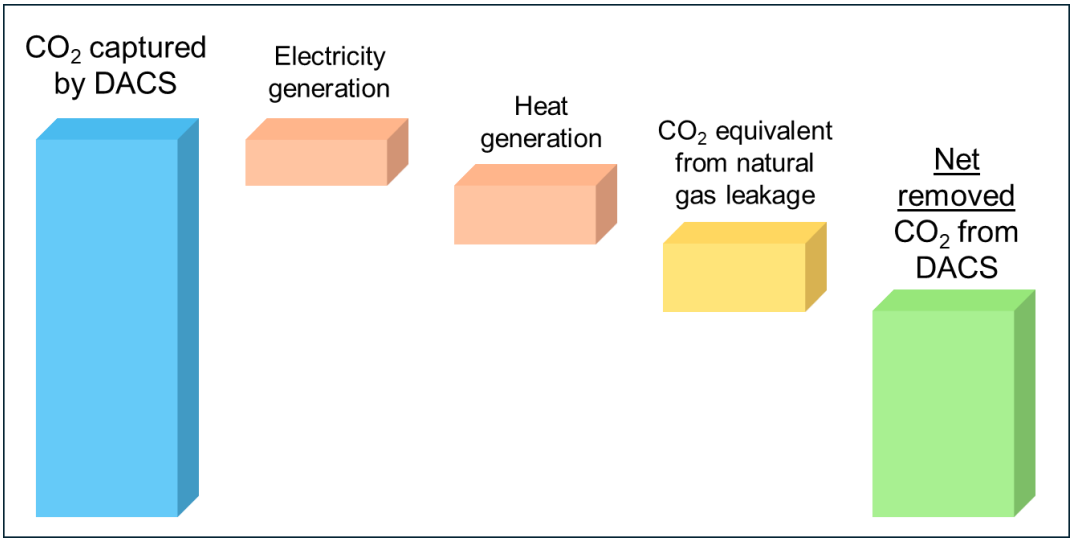

Figure S2. Illustration of 'net-removed' CO_2 in a typical adsorbent DACS process utilizing either grid or renewable resources for electricity requirements, and combustion of natural gas for heat requirements. This illustration assumes no capture of CO_2 released from electricity and heat generation alongside direct air capture of CO_2 from the atmosphere. In some cases, calculating net CO_2 removal may result in a negative number, in which case the DACS process results in net CO_2 emissions.

Table S2. United States state-specific electricity prices and carbon intensities.

State	2025 electricity purchase price [US$/kWh][a]	2025 grid carbon intensity [gCO_2/kWh][b]	2050 electricity purchase price [US$/kWh][c]
Alabama	7.21	538	9.22
Alaska	19.20	347	21.70
Arizona	7.74	483	8.00
Arkansas	7.49	315	7.47
California	16.89	228	9.38
Colorado	9.13	547	5.38
Connecticut	10.97	248	12.96
Delaware	8.66	571	12.71
D.C.	8.97	531	10.14
Florida	8.72	390	10.43
Georgia	7.40	350	10.60
Hawaii	30.90	699	34.93
Idaho	7.28	152	8.91
Illinois	8.32	314	8.14
Indiana	8.42	747	8.75
Iowa	7.56	430	6.73
Kansas	8.41	401	5.72
Kentucky	6.78	801	9.94
Louisiana	7.08	464	8.03
Maine	10.88	209	11.55
Maryland	9.64	314	12.16
Massachusetts	17.30	430	12.65
Michigan	8.76	475	9.09
Minnesota	9.45	391	6.55
Mississippi	6.78	378	8.30
Missouri	8.10	774	7.12
Montana	7.11	511	7.66
Nebraska	8.27	559	5.71
Nevada	6.86	332	8.70
New Hampshire	15.74	131	12.18
New Jersey	12.19	240	12.97
New Mexico	7.02	488	5.00
New York	7.22	226	11.48
North Carolina	7.00	317	10.53
North Dakota	8.40	640	4.51
Ohio	7.46	547	10.11
Oklahoma	6.27	344	6.06

State	2025 electricity purchase price [US$/kWh][a]	2025 grid carbon intensity [gCO_2/kWh][b]	2050 electricity purchase price [US$/kWh][c]
Oregon	6.80	142	9.42
Pennsylvania	7.45	331	11.77
Rhode Island	18.30	381	12.78
South Carolina	6.92	255	9.97
South Dakota	9.14	145	5.53
Tennessee	6.28	342	9.18
Texas	6.97	427	6.63
Utah	7.05	697	8.11
Vermont	12.97	4.99	11.00
Virginia	7.40	294	11.62
Washington	6.62	99.3	9.76
West Virginia	6.92	877	10.92
Wisconsin	8.69	565	7.82
Wyoming	7.78	843	5.44
United States average	9.41	388	6.51

[a] U.S. Energy Information Administration, EIA-861, 2021, Total Electric Industry, Industrial price [5], projected to 2025 from 2021 (14% increase)

[b] U.S. Energy Information Administration, 2021, Table 7. Electric power industry emissions estimates [6]

[c] NREL, Cambium 2022, Mid-case with 100% decarbonization by 2035, 2050 projected [7]. United States average is a weighted average of state-level 2050 projected electricity prices by potential renewable generation capacity.

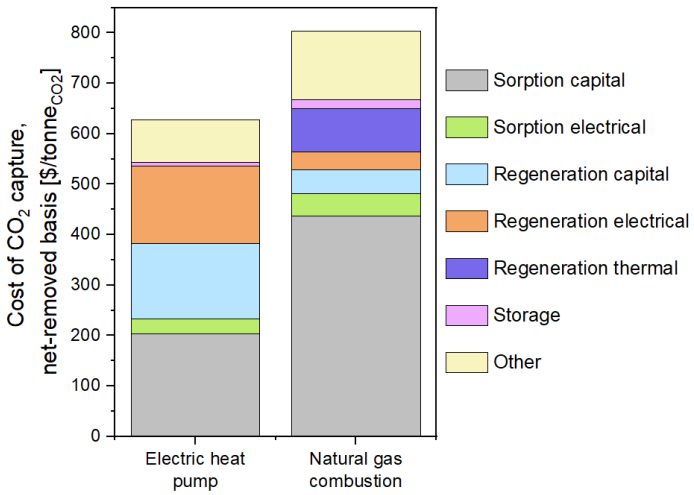

Figure S3. Cost breakdowns for first-of-a-kind adsorbent DACS facilities, utilizing either an electric heat pump or natural gas combustion to provide thermal energy for regeneration. Costs, calculated on a 'net-removed CO_2' basis, assume facility size of 0.3 megatonnes CO_2 per year.

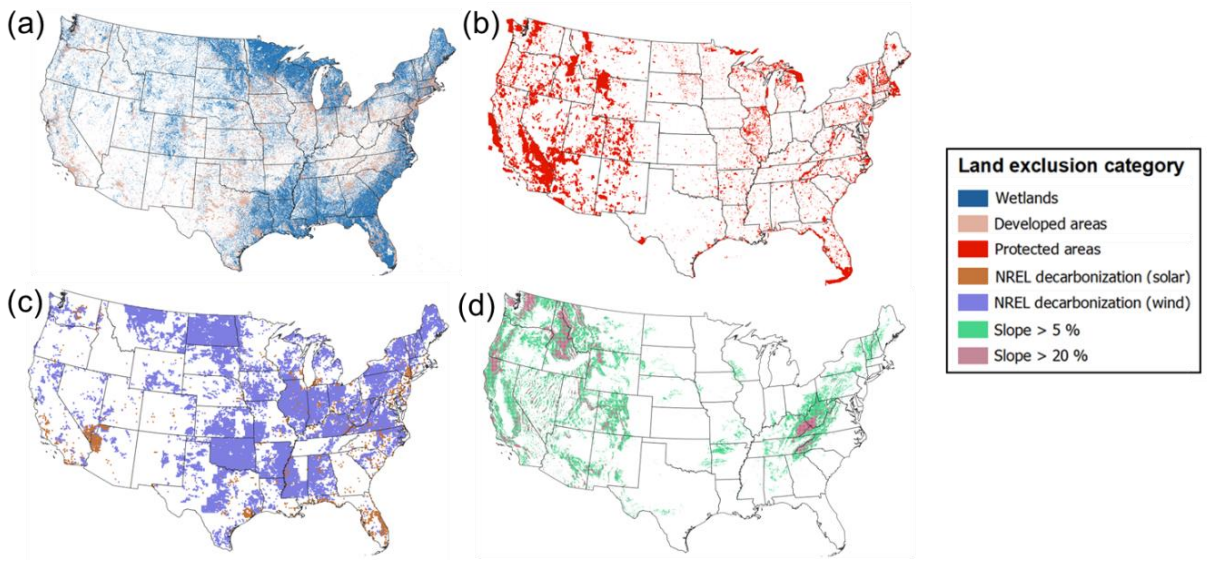

Figure S4. Maps illustrating land exclusions applied to renewable electricity deployment for adsorbent DACS: (a) wetlands and developed area buffers; (b) protected areas; (c) lands prioritized for grid decarbonization, based on analyses by the National Renewable Energy Laboratory [8]; (d) land slopes exceeding allowable values for wind and solar deployment.

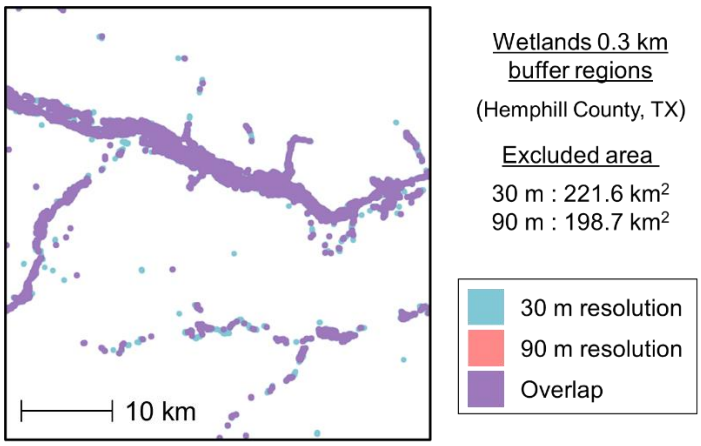

Figure S5. Land excluded by the wetland buffer condition using 30-meter (blue) and 90-meter (red) resolution in Hemphill County, Texas, including overlap between the two regions (purple).

The resolution of the geospatial analysis can have several impacts on the determined quantity of suitable land. First, pixels of 'unsuitable' land use classes that would be excluded from use, due to merging with neighboring pixels, remain in the dataset. As a result, more pixels/land are identified as not suitable due to the land cover type. This results in a higher level of fragmentation in the land and more potential discontinuity, reducing the quantity of contiguous land. Additionally, the slope calculated can vary based on the resolution. Buakhao and Kangrang [9] found that, for the same area, the slope calculated at 90-meter resolution is 25% percent lower than the slope calculated at 30-meter resolution. Finally, roads, railways, and low-voltage transmission lines disappear at lower resolutions and are therefore not properly accounted for. The retention of smaller land class features at higher resolutions leads to more exclusions based on the 5 km^2 contiguous land condition compared to lower resolution. These factors result in a more conservative estimate of the quantity of suitable land for electricity generation.

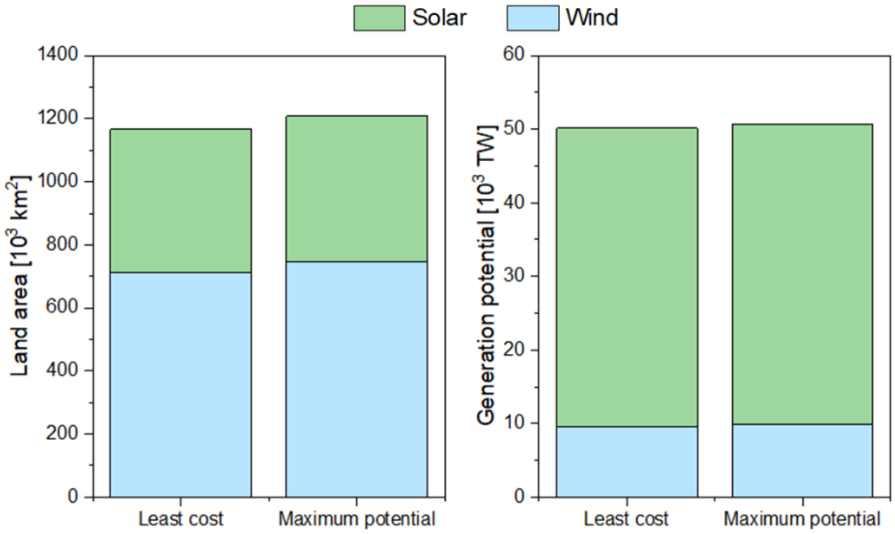

Figure S6. Impact of selecting grid-level electricity generation technology based on least cost vs. maximum generation potential. Similar results are obtained when comparing land use, generation potential, and median cost of electricity.

Levelized costs of energy (LCOE) were calculated using the Electricity Annual Technology Baseline's 2050 Moderate scenario [10]. Spatially explicit estimates of LCOE were based on resource class (**Table S3, S4**), i.e. wind speed at a 120-meter height and global horizontal irradiance for wind and solar electricity respectively [11,12].

Table S3. Criteria applied for land suitability of wind and solar deployment for DACS.

Condition	Notes	Data Source
NLCD	Open water excluded	[13]
Protected land	Protected Areas Database, National Conservation Easement Database 3 km buffer distance for GAP[a]-status = 1, 2 (e.g., national parks 0 km buffer distance for GAP[a]-status = 3, 4 (e.g., state parks)	[14,15]
	3 km buffer distance for areas of critical environmental concern	[16]
	3 km buffer distance for roadless areas	[17]
Wetlands	0.3 km buffer distance	[13]
Developed	0 km buffer distance	[13]
Other developed	Airports: 3 km buffer distance	[18]
	Railroads: 0.015 km buffer distance	[18]
	Transmission lines: buffer distance based on voltage	[18]
	Power plants: 3 km buffer distance	[19]
	Buildings: 0.3 km buffer distance	[20]
	Wind turbines: 3 km buffer distance	[21]
Decarbonization	Excluded land overlapping with prioritized renewable electricity development area	[8]
Slope (Solar)	Slope <5% (2.86°)	[22]
Slope (Wind)	Slope <20% (11.31°)	[22]
Co-location (Solar)	Excluded lands with forests, pasture/hay or cultivated crops occupying >25% of ~5 km^2 grid space	[13]
Co-location (Wind)	Excluded lands with forests occupying >25% of ~5 km^2 grid space	[13]
Contiguity	<5 km^2 contiguous area excluded	Calculated

[a] GAP = Gap Analysis Project

Table S4: Land-based wind resource classes and levelized cost of electricity [10].

Type	Min. wind speed [m/s]	Max. wind speed [m/s]	LCOE [$/MWh]
Class 1	9.01	12.89	15.4
Class 2	8.77	9.01	16.6
Class 3	8.57	8.77	17.0
Class 4	8.35	8.57	17.5
Class 5	8.07	8.35	18.0
Class 6	7.62	8.07	18.9
Class 7	7.10	7.62	20.8
Class 8	6.53	7.10	23.3
Class 9	5.90	6.53	27.9
Class 10	1.72	5.90	42.5

Table S5: Utility-scale solar photovoltaic resource classes and levelized cost of electricity [10]

Type	Min. GHI [a] [kWh/m^2/day]	Max. GHI [kWh/m^2/day]	LCOE [$/MWh]
Class 1	5.75	-	13.2
Class 2	5.50	5.75	13.6
Class 3	5.25	5.50	14.3
Class 4	5.00	5.25	15.1
Class 5	4.75	5.00	16.1
Class 6	4.50	4.75	16.8
Class 7	4.25	4.5	17.6
Class 8	4.00	4.25	18.5
Class 9	3.75	4.00	19.4
Class 10	0	3.75	21.2

[a] Global horizontal irradiance

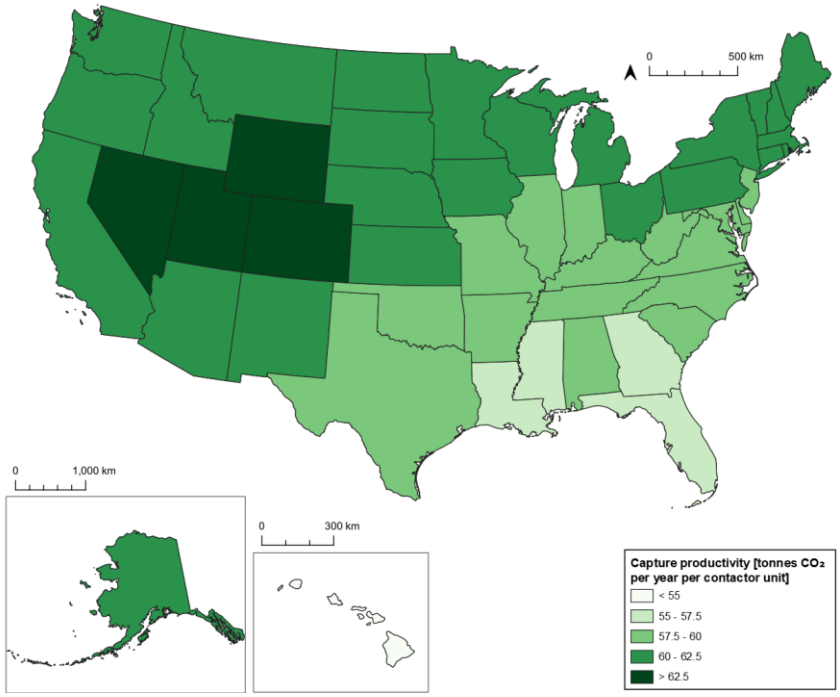

Figure S7. State-level CO_2 capture productivities, defined per adsorbent contactor unit, illustrating impact of local temperature and dew point on DACS performance.

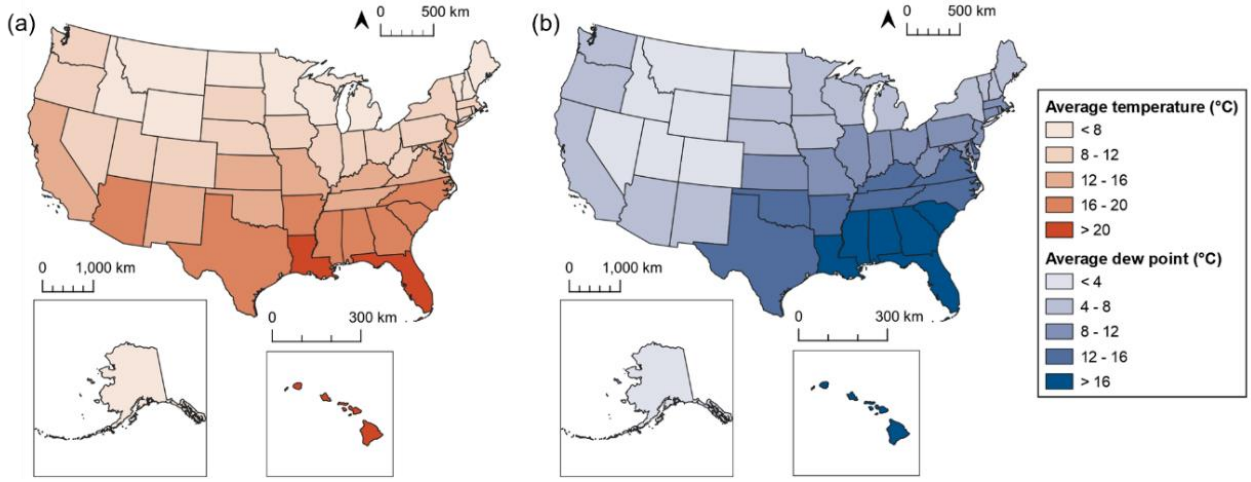

Figure S8: State-level (a) temperature and (b) dew point [23].

The focus of this study is capture based on an amine-based adsorbent, but it is important to note that different capture technologies have different responses to local climate conditions. For example, physisorbents perform poorly in humid conditions due to competition between water and

CO_2 for active sites, but may be suitable for cold, dry conditions such as Alaska [24]. Optimizing productivity through the selection of adsorbents or process variables tailored to specific environments could have significant impacts on both capture capacity and cost [25], but is outside the scope of this work. Another topic warranting additional study is that many regions experience significant changes to temperature and humidity throughout the year, and even throughout a single 24-hour period. As adsorbent DAC processes typically operate with total cycle times less than one hour changes in local conditions during a regular diurnal cycle could impact performance by up to a factor of ~2 [26].

Table S6. State-level building cost coefficients.

State	Average cost factor [a]	State	Average cost factor [a]
Alabama	0.835	Montana	1.084
Alaska	2.718	Nebraska	0.913
Arizona	0.935	Nevada	1.150
Arkansas	0.910	New Hampshire	1.080
California	1.205	New Jersey	1.192
Colorado	1.037	New Mexico	0.933
Connecticut	1.136	New York	1.127
Delaware	1.121	North Carolina	0.879
D.C.	1.04	North Dakota	1.118
Florida	0.858	Ohio	0.961
Georgia	0.859	Oklahoma	0.909
Hawaii	2.175	Oregon	1.168
Idaho	0.988	Pennsylvania	1.090
Illinois	1.078	Rhode Island	1.138
Indiana	0.916	South Carolina	0.926
Iowa	0.988	South Dakota	0.982
Kansas	0.911	Tennessee	0.846
Kentucky	0.914	Texas	0.894
Louisiana	0.887	Utah	1.093
Maine	1.077	Vermont	1.001
Maryland	0.995	Virginia	0.973
Massachusetts	1.180	Washington	1.142
Michigan	1.021	West Virginia	0.972
Minnesota	1.102	Wisconsin	1.092

Mississippi	0.798		Wyoming	1.022
Missouri	0.949			

[a] US DoD Facilities Pricing Guide (UFC 3-701-01) [27]. Average of area cost factors by state (Table 4-1, CONUS).

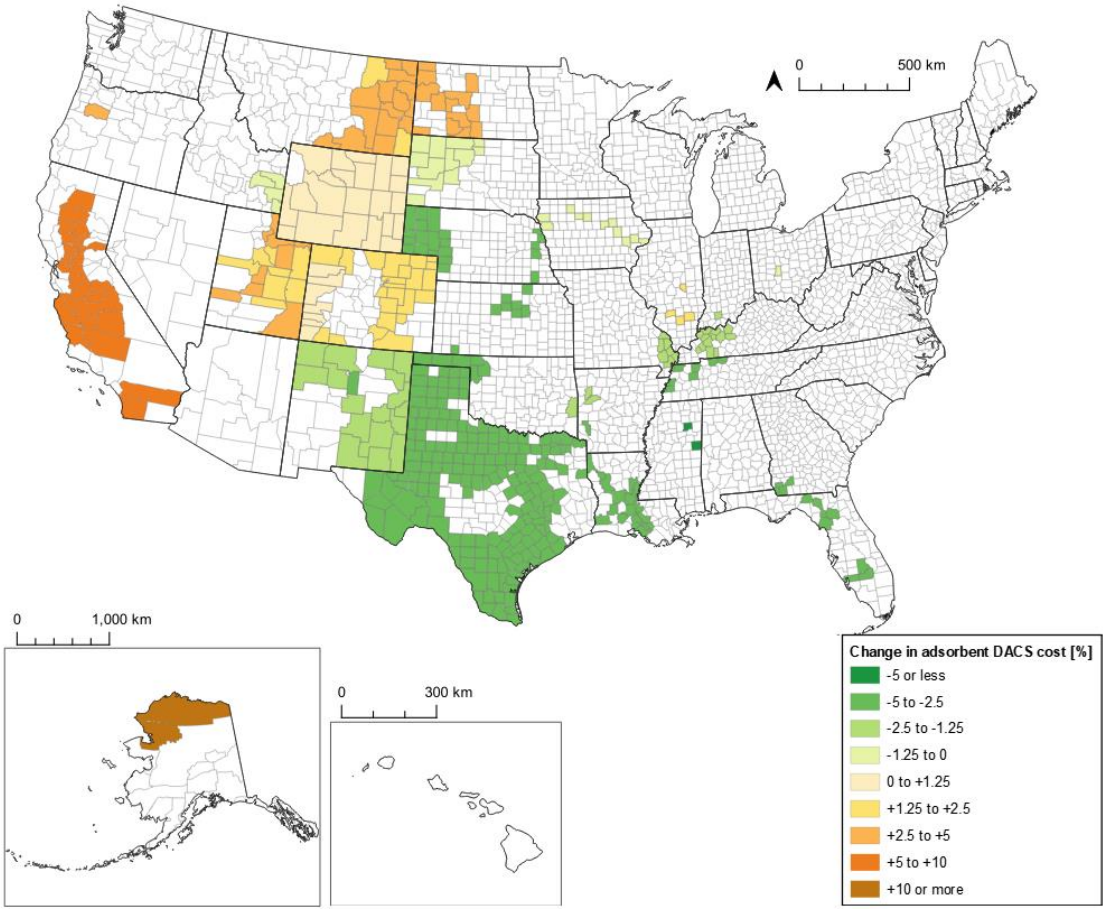

Figure S9. Percent change in total cost for adsorbent DACS in 2050 after applying state-specific cost factors.

State-level building costs were also considered for their impact on capture cost [27]. Generally, there was a strong correlation between state-level electricity and building costs. Many of the identified 'high priority' regions had cost coefficients between 0.85-1.15, resulting in minimal positive or negative changes to DACS cost. The primary exception to this is Alaska with a coefficient of 2.7, which resulted in an average increase in capture cost of 29%, or $133 per tonne of CO_2.

Potential for utilizing geothermal heat for adsorbent DACS

There is potential for using low-grade (70–150 °C) geothermal brine to upgrade process steam, thereby reducing the electricity requirements of the process heat pump compared to an air-source heat pump. To understand the impact on cost and capacity, the adsorbent DACS process was modelled using a heat pump with a coefficient of performance of 4 to reflect the increased heat source temperature. Heat from the resource, assumed to be re-injected at a temperature of 70 °C, was upgraded to produce steam using a heat pump. Yearly DACS capacity utilizing heat from hydrothermal sources was calculated using the following equations:

$$Capacity_{Geo\ Ad-DAC} = \frac{Q_{steam}}{\left(E_{steam}/tonne_{CO_2}\right)}$$

$$Q_{steam} = Q_{hydrothermal} \times \frac{COP_{HP}}{COP_{HP} - 1}$$

$$COP_{HP} = \frac{Q_{steam}}{W_{in}} = \frac{Q_{hydrothermal} + W_{in}}{W_{in}} = 4$$

where Q_{steam} is the quantity of thermal energy produced by the hydrothermal-source heat pump in GJ per year, $E_{steam}/tonne_{CO2}$ is the thermal energy requirement of adsorbent DACS process in GJ per tonne of CO_2, $Q_{hydrothermal}$ is the thermal energy available in the hydrothermal resource in GJ per year (assuming a re-injection temperature of 70 °C, calculated using the resource temperature and flow rate), and W_{in} is the heat pump work input, as electrical energy in GJ per year. Resource temperatures and flow rates were obtained from the NREL Geothermal Prospector [28]. Resources with temperatures exceeding 150 °C were not considered due to their potential for electricity generation [29] and grid decarbonization [30]. Adsorbent DACS was calculated for a facility scale determined by the availability of thermal energy for each hydrothermal resource, with a

minimum of 10 kilotonnes of CO_2 per year, and a levelized cost of hydrothermal heat, determined using the System Advisory Model [31].

Hydrothermal resources with known temperature and flow-rate information [28] could provide thermal energy to power nearly 2.1 million tonnes per year of adsorbent DAC (**Figure S7**) at costs between $240–460 per tonne of CO_2, with an average of $285 per tonne of CO_2. The majority of these resources are located within the western United States. Capture cost was strongly influenced by the temperature of the hydrothermal resource and the scale of the facility, and did not include storage costs due to the lack of overlap between hydrothermal resources and storage with quantifiable cost. A 2023 analysis [32] suggests that harnessing geothermal energy in Texas, California, or Alaska could result in capture costs 16–33 % lower than baselines utilizing grid electricity, with carbon intensities similar to those in **Figure 3** in the main text, to drive regeneration. In this work, utilization of hydrothermal resources would either require some form of CO_2 transportation or an alternative CO_2 end case, e.g. utilization or conversion, both of which are outside the scope of this study.

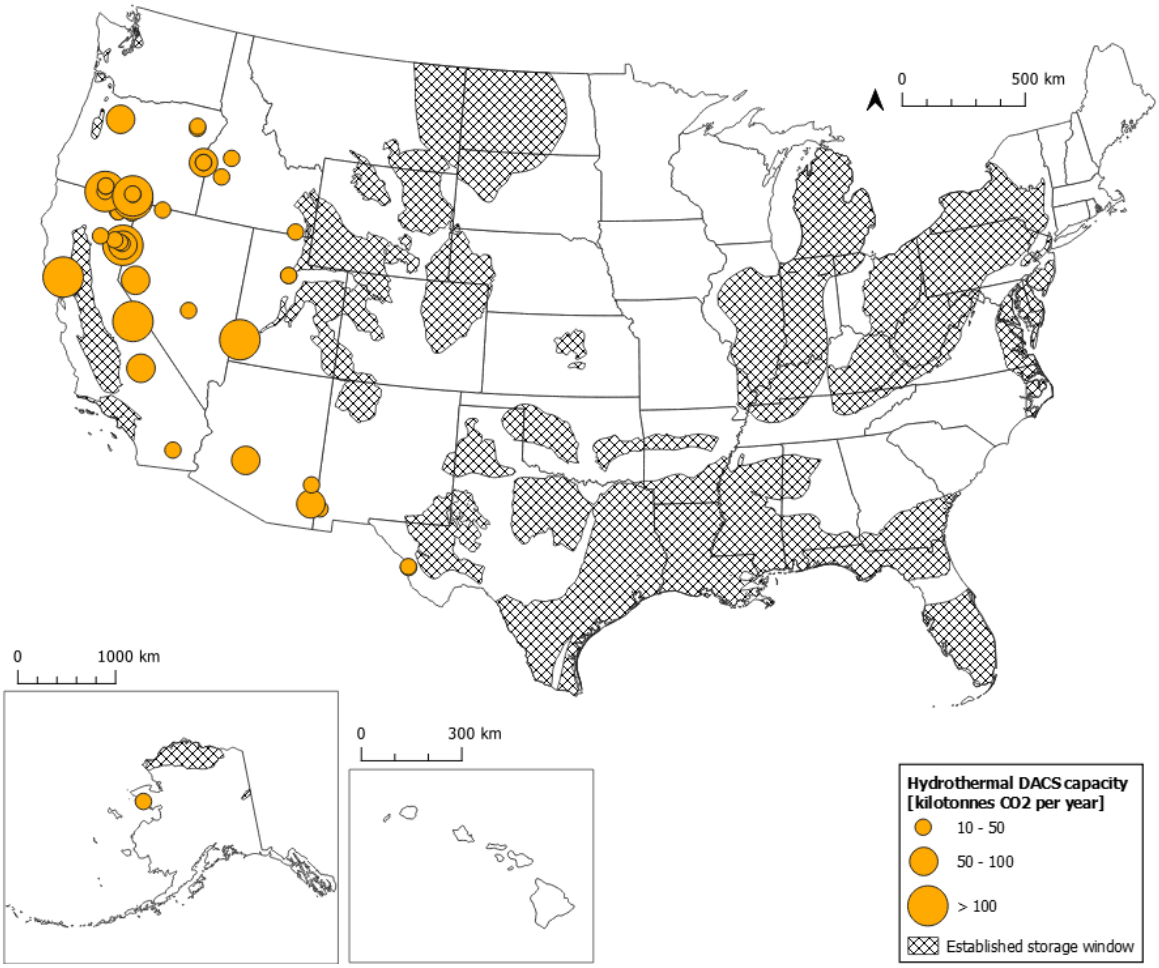

Figure S10: Potential for adsorbent DACS in 2050, where thermal energy requirements are provided for at least partially by hydrothermal resources 70–150 °C.

References

(1) McQueen, N.; Psarras, P.; Pilorgé, H.; Liguori, S.; He, J.; Yuan, M.; Woodall, C. M.; Kian, K.; Pierpoint, L.; Jurewicz, J.; Lucas, J. M.; Jacobson, R.; Deich, N.; Wilcox, J. Cost Analysis of Direct Air Capture and Sequestration Coupled to Low-Carbon Thermal Energy in the United States. *Environ. Sci. Technol.* **2020**, *54* (12), 7542–7551. https://doi.org/10.1021/acs.est.0c00476.

(2) Sinha, A.; Realff, M. J. A Parametric Study of the Techno-economics of Direct CO_2 Air Capture Systems Using Solid Adsorbents. *AIChE J.* **2019**, *65* (7). https://doi.org/10.1002/aic.16607.

(3) Zoelle, A.; Keairns, D.; Pinkerton, L.; Turner, M.; Woods, M.; Kuehn, N.; Shah, V.; Chou, V. *Cost and Performance Baseline for Fossil Energy Plants Volume 1a: Bituminous Coal (PC) and Natural Gas to Electricity Revision 3*; DOE/NETL-2015/1723, 1480987; 2015; p DOE/NETL-2015/1723, 1480987. https://doi.org/10.2172/1480987.

(4) Deutz, S.; Bardow, A. Life-Cycle Assessment of an Industrial Direct Air Capture Process Based on Temperature–Vacuum Swing Adsorption. *Nat Energy* **2021**, *6* (2), 203–213. https://doi.org/10.1038/s41560-020-00771-9.

(5) U.S. Energy Information Administration (EIA). EIA-861 Annual Electric Power Industry Report: Annual Sales to Ultimate Customers by State and Sector (2010-2022), 2023. https://www.eia.gov/electricity/data/state/.

(6) U.S. Energy Information Administration (EIA). State Electricity Profiles (2021), 2022. https://www.eia.gov/electricity/state/archive/2021/.

(7) Gagnon, P.; Cowiestoll, B.; Schwarz, M. *Cambium 2022 Scenario Descriptions and Documentation*; NREL/TP-6A40-84916; National Renewable Energy Laboratory, 2023. https://www.nrel.gov/research/publications.

(8) Denholm, P.; Brown, P.; Cole, W.; Mai, T.; Sergi, B.; Brown, M.; Jadun, P.; Ho, J.; Mayernik, J.; McMillan, C.; Sreenath, R. *Examining Supply-Side Options to Achieve 100% Clean Electricity by 2035*; NREL/TP-6A40-81644, 1885591, MainId:82417; 2022; p NREL/TP-6A40-81644, 1885591, MainId:82417. https://doi.org/10.2172/1885591.

(9) Buakhao, W.; Kangrang, A. DEM Resolution Impact on the Estimation of the Physical Characteristics of Watersheds by Using SWAT. *Advances in Civil Engineering* **2016**, *2016*, 1–9. https://doi.org/10.1155/2016/8180158.

(10) National Renewable Energy Laboratory. *Annual Technology Baseline*. https://atb.nrel.gov/ (accessed 2024-02-20).

(11) National Renewable Energy Laboratory. Wind Supply Curves. https://www.nrel.gov/gis/wind-supply-curves.html (accessed 2023-04-11).

(12) National Renewable Energy Laboratory. Solar Supply Curves. https://www.nrel.gov/gis/solar-supply-curves.html (accessed 2023-04-11).

(13) Dewitz, J.; U.S. Geological Survey. National Land Cover Database (NLCD) 2019 Products (Ver. 2.0), 2021. https://doi.org/10.5066/P9KZCM54.

(14) National Conservation Easement Database | NCED. https://www.conservationeasement.us/ (accessed 2023-04-11).

(15) U.S. Geological Survey (USGS); Gap Analysis Project (GAP). Protected Areas Database of the United States (PAD-US) 3.0 (Ver. 2.0, March 2023), 2022. https://doi.org/10.5066/P9Q9LQ4B.

(16) Bureau of Land Management. Areas of Critical Environmental Concern. https://www.blm.gov/programs/planning-and-nepa/planning-101/special-planning-designations/acec (accessed 2023-04-11).
(17) USDA Forest Service. USDA Forest Service FSGeodata Clearinghouse- Download National Datasets. https://data.fs.usda.gov/geodata/edw/datasets.php (accessed 2023-04-11).
(18) U.S. Department of Homeland Security. Homeland Infrastructure Foundation-Level Data (HIFLD). https://hifld-geoplatform.opendata.arcgis.com/ (accessed 2023-04-11).
(19) U.S. Energy Information Administration (EIA). Power Plants, 2023. https://atlas.eia.gov/maps/power-plants (accessed 2023-05-11).
(20) Microsoft Corporation. Microsoft Maps- US Building Footprints, 2023. https://github.com/microsoft/USBuildingFootprints (accessed 2023-04-11).
(21) Rand, J. T.; Kramer, L. A.; Garrity, C. P.; Hoen, B. D.; Diffendorfer, J. E.; Hunt, H. E.; Spears, M. A Continuously Updated, Geospatially Rectified Database of Utility-Scale Wind Turbines in the United States. *Sci Data* **2020**, *7* (1), 15. https://doi.org/10.1038/s41597-020-0353-6.
(22) Jarvis, A.; Guevara, E.; Reuter, H. I.; Nelson, A. D. *Hole-filled SRTM for the globe : version 4 : data grid*. CGIAR Consortium for Spatial Information. http://srtm.csi.cgiar.org/ (accessed 2023-07-11).
(23) NASA Center For Climate Simulation. NASA Earth Exchange Global Daily Downscaled Projections (NEX-GDDP-CMIP6), 2021. https://doi.org/10.7917/OFSG3345.
(24) Wilson, S. M. W. The Potential of Direct Air Capture Using Adsorbents in Cold Climates. *iScience* **2022**, *25* (12), 105564. https://doi.org/10.1016/j.isci.2022.105564.
(25) Cai, X.; Coletti, M. A.; Sholl, D. S.; Allen-Dumas, M. R. Assessing Impacts of Atmospheric Conditions on Efficiency and Siting of Large-Scale Direct Air Capture Facilities. *JACS Au* **2024**, *4* (5), 1883–1891. https://doi.org/10.1021/jacsau.4c00082.
(26) Sendi, M.; Bui, M.; Mac Dowell, N.; Fennell, P. Geospatial Analysis of Regional Climate Impacts to Accelerate Cost-Efficient Direct Air Capture Deployment. *One Earth* **2022**, *5* (10), 1153–1164. https://doi.org/10.1016/j.oneear.2022.09.003.
(27) U.S. Department of Defense. UFC 3-701-01 DoD Facilities Pricing Guide, with Change 3 | WBDG - Whole Building Design Guide. https://www.wbdg.org/ffc/dod/unified-facilities-criteria-ufc/ufc-3-701-01 (accessed 2023-04-11).
(28) Getman, D.; Anderson, A.; Augustine, C. Geothermal Prospector: Supporting Geothermal Analysis Through Spatial Data Visualization and Querying Tools. In *Proceedings of the Geothermal Resources Council 2015 Annual Meeting*; Reno, NV, 2015.
(29) U.S. Energy Information Administration (EIA). *Geothermal explained- Geothermal power plants*. https://www.eia.gov/energyexplained/geothermal/geothermal-power-plants.php (accessed 2024-08-02).
(30) Vargas, C. A.; Caracciolo, L.; Ball, P. J. Geothermal Energy as a Means to Decarbonize the Energy Mix of Megacities. *Commun Earth Environ* **2022**, *3* (1), 66. https://doi.org/10.1038/s43247-022-00386-w.
(31) Blair, N.; DiOrio, N.; Freeman, J.; Gilman, P.; Janzou, S.; Neises, T.; Wagner, M. *System Advisor Model (SAM) General Description (Version 2017.9.5)*; Technical Report NREL/TP-6A20-70414; National Renewable Energy Laboratory, 2018. https://doi.org/10.2172/1440404.

(32) Kuru, T.; Khaleghi, K.; Livescu, S. Solid Sorbent Direct Air Capture Using Geothermal Energy Resources (S-DAC-GT) – Region Specific Analysis. *Geoenergy Science and Engineering* **2023**, *224*, 211645. https://doi.org/10.1016/j.geoen.2023.211645.